Supplementary Information (SI) for Polymer Chemistry.
This journal is © The Royal Society of Chemistry 2026

Supporting information

Poly(chromenochromenedione) (PCCD): a Structural Isomer of Poly(benzodifurandione) (PBDF)

Uttam Pal,[a] Reed M. Woolard,[a] Priyanka Rout,[a] Sanket Samal,[a] Suman Kuila,[b] Md Masudur Rahman Rahat,[a] Guancheng Shen,[c] Juila Laskin,[a] Stephen Barlow,[b] Seth R. Marder,[b,d] Geoffrey R. Hutchison,[c,e] Jianguo Mei [a]*

[a] James Tarpo Jr. and Margaret Tarpo Department of Chemistry, Purdue University, West Lafayette, Indiana 47907, USA. E-mail: jgmei@purdue.com

[b] Renewable and Sustainable Energy Institute, University of Colorado Boulder, Boulder, Colorado 80309, USA.

[c] Department of Chemistry, University of Pittsburgh, Pittsburgh, Pennsylvania 15260, USA.

[d] Department of Chemistry and of Chemical and Biological Engineering, University of Colorado Boulder, Boulder, Colorado 80309, USA.

[e] Department of Chemical and Petroleum Engineering, University of Pittsburgh, Pittsburgh, Pennsylvania 15261, USA.

Materials

All reagents and solvents used for synthesis and analysis were purchased from Sigma-Aldrich, Alfa Aesar, Thermo Fisher, and TCI, and were used without further purification unless otherwise noted. All reactions were carried out under a nitrogen atmosphere unless mentioned otherwise.

Sample Preparation

PPDA thin film formation: Glass substrates (20 mm × 20mm) were cleaned with sequential sonication steps in soap water, deionized water, acetone, and isopropyl alcohol for 15 min each and then they were dried by a nitrogen gun. The cleaned glass substrates were exposed to UV-ozone treatment (HELIOS-500 Ultraviolet-Ozone Cleaner) for 20 min to increase surface hydrophilicity and remove any organic residue. PPDA water solution (8mg/ml) was used to deposit PPDA thin films on the glass substrate via spin-coating method at 2000 rpm for 20 s. After spin coating the thin films were air dried for 20 min followed by vacuum drying for 30 min to ensure complete water removal. After the in-situ conversion of PPDA to PCCD, the thickness was measured to be approximately 40 nm.

n-PCCD thin film preparation: ITO-coated glass substrates were sequentially cleaned by ultrasonication in deionized water, acetone, and isopropanol for 15 min each, followed by oven drying. The substrates were then treated with UV–ozone (Jelight UVO cleaner) for 20 minutes prior to film deposition to remove residual organic contaminants and enhance surface hydrophilicity. The n-PCCD (50 wt% N-DMBI$^+$) thin films were deposited on ITO via an off-center spin-coating method at 1500 rpm for 60 s, followed by 3000 rpm for 10 s per layer. This deposition cycle was repeated six times to obtain a total thickness of approximately 96 nm. After each layer, the films were dried in a vacuum oven for 1 hour to ensure complete solvent removal and uniform coating.

Sequential doping of in situ converted PCCD films: PPDA aqueous solution (5 mg/mL) was drop-cast onto precleaned, UV–ozone treated glass substrates (1 cm × 1 cm). The films were dried in a vacuum oven at 40 °C for 6 h. The dried films were then exposed to HCl vapor at 90 °C for 20 min, followed by thermal annealing at 180 °C for 1 h. After cooling to 90 °C, concentrated HCl (100 µL) was directly added to the films to facilitate ring closing in the drop-cast films (~400 nm), and the films were allowed to dry at that temperature. After drying, the films were further annealed at 180 °C for 3 h to complete the conversion to PCCD.

A 2 mM N-DMBI$_2$ solution in DMSO was prepared by heating at 60 °C for 20 min in a nitrogen-filled glovebox. The solution (100 µL) was drop cast onto the PCCD thin films, followed by thermal annealing at 140 °C for 5 min. After the films dried, an additional 100 µL of the N-DMBI$_2$ solution was added, and the films were dried again and annealed at 140 °C for 30 min. The sheet resistance was then measured using a four point probe instrument.

Characterizations

NMR Spectroscopy: NMR experiments were conducted with Bruker AV 400 MHz AVANCE III HD and Bruker NEO500-1 spectrometers using Topspin 3.2 Software. The solid state ^{13}C CP-MAS spectra were obtained on a Chemagnetics CMX-400 NMR spectrometer running SpinSight software and equipped with a wide-bore magnet and a 5mm triple-resonance (H-X-Y) MAS probe. The pulse sequence used was the "cp_tppm" sequence from the spectrometer's pulse program library. Acquisition parameters included ^{1}H and ^{13}C RF field strengths of 56 KHz, a cross-polarization time of 2 ms, a relaxation delay of 6 seconds, a data acquisition time of 32 ms with a sweep width of 32 KHz, and a sample spinning rate of 5.6 KHz. Typically, 8192 scans were acquired (experiment time of ca. 14 hours) and the data was processed with exponential multiplication (line-broadening of 48 Hz.) and zero-filled twice prior to Fourier transformation. The chemical shifts were externally referenced using a sample of glycine with the downfield ^{13}C resonance set to +176.4 ppm.

ATR-FTIR Spectroscopy: FTIR spectra of the small oligomers in powder form and polymer system in drop casted films on glass substrates were obtained using a Thermo Nicolet 6700 FTIR spectrometer on a Diamond ATR setup.

Raman Spectroscopy: A 532 nm single longitudinal mode laser (CNI Laser) with a maximum output power of 200 mW is used as the excitation source. The laser was focused onto the sample using a 63x air objective lens (Leica, HI PLAN 63x/0,75) with an incident power of 60 mW. The Raman signal was collected in the reflection direction. The spRS spectral acquisition was carried out using a Kymera 328i spectrograph paired with an EMCCD (Newton 920, 1024×256 pixels, Oxford Instruments), which was cooled to -80°C to reduce thermal noise during acquisition. To block the 532 nm excitation laser effectively, a long pass filter was placed before the 80 μm spectrometer entrance slit. Signal dispersion was accomplished using a 600 lines/mm grating within the spectrometer. The spectral acquisition process was achieved through Solis software (Oxford Instruments).

UV–Vis–NIR Absorption Spectroscopy: Absorption spectra were recorded using an Agilent Cary 5000/6000i UV–Vis–NIR spectrophotometer (Cary WinUV software). Solution-phase spectra were measured at a concentration of 0.05 mM in a quartz cuvette with a 1 cm path length.

ESI–Mass Spectrometry (ESI-MS): Mass spectrometric measurements were conducted using an Agilent 6560 Ion Mobility Quadrupole Time-of-Flight (IM Q-TOF) mass spectrometer (Santa Clara, CA, USA) equipped with a custom-designed electrospray ionization (ESI) source. A 1000 μM solution of the sample was infused into the instrument at a flow rate of 1 μL/min using a fused-silica capillary (50 μm ID, 150 μm OD). The ESI conditions included a spray voltage of –3.5 kV and an inlet temperature of 250 °C. Spectra were acquired in negative ion mode over an m/z range of 100–3200 with a resolving power (m/Δm) of 25,000 at m/z 751. The solvent used was an 80:20 (v/v) mixture of acetonitrile and DMSO.

Electron Paramagnetic Resonance (EPR): EPR measurements of solid small oligomer and its doped states were measured at room temperature on a Bruker EMX EPR Spectrometer using Win EPR Acquisition Software. EPR measurements of the doped and neutral polymer solutions in DMSO (8 mg/ml) were obtained at 20 K on a Bruker EMX EPR Spectrometer using Win EPR Acquisition Software.

Thin film thickness and surface morphology: Characterization were performed via atomic force microscopy (AFM) using a Bruker iCON Dimension in tapping mode to enable non-destructive topography analysis. For films exceeding 100 nm in thickness, a surface profilometer (DektakXT, Bruker) was employed. Thickness measurements were performed at a minimum of three distinct points across multiple substrate batches to ensure reliability and reproducibility under consistent processing conditions.

A 2mM (N-DMBI$_2$) DMSO solution was prepared by heating at 60 C for 20 min in a nitrogen filled glovebox. 100 miro lit of this solution was drop casted in to the PCCD thin films followed by thermal anneling at 140 c when the films get dried another 100 micro lit solution was added to the film dried again and left anneling for 30 min. then the sheet resistance was measured using the 4 point probe instrument.

Electrochemical and Spectro Electrochemical Measurements: Electrochemical measurements were carried out in a three-electrode quartz cuvette cell using a leakless Ag/AgCl reference electrode (eDAQ Inc.) and a platinum wire counter electrode (0.5 mm diameter, >99.99% metals basis, Thermo Scientific Chemicals). Ferrocene/ferrocenium (Fc/Fc^+) was used as an external standard to calibrate the reference electrode potential. The electrolyte consisted of 0.2 M tetrabutylammonium bis(trifluoromethanesulfonyl)imide (TBA-TFSI) dissolved in anhydrous propylene carbonate (PC), prepared inside an N_2-filled glovebox with H_2O and O_2 levels maintained below 0.1 ppm. Cyclic voltammetry (CV) measurements were performed inside a

Faraday cage using a VSP multichannel potentiostat (BioLogic Inc.) and analyzed with EC-Lab software. Prior to data acquisition, film electrodes were conditioned by repeated CV cycling (minimum of five cycles) within a potential window of −0.4 V to 0.8 V until stable and reproducible voltammograms were obtained. Spectroelectrochemical measurements were performed in a quartz cuvette using a Cary 5000 UV–Vis–NIR spectrometer (Agilent Inc.) coupled with an SP-150 potentiostat (BioLogic Inc.) after electrochemical conditioning of the films. A bare ITO/glass substrate placed in an identical cuvette containing the same electrolyte was used to record the baseline spectrum. Distinct electrochemical doping states were induced by applying chronoamperometry (CA) at selected potentials for 3 minutes each, during which the corresponding spectra were recorded concurrently.

Conductivity and Sheet Resistance Measurements: Drop-cast films of doped polymer solutions were prepared for the analysis of electrical performance. A Filmetrics R50 Sheet Resistance Mapper was used to measure the thin films' sheet resistance using a four-probe configuration. In the four-probe configuration, the sheet resistance was then measured using following equation based on previously reported literature.[1]

$$R_s = \frac{w}{l} \times \frac{\Delta V}{I} = 10\frac{\Delta V}{I} \qquad (1)$$

The conductivities were then calculated using the following equation:

$$\sigma = \frac{1}{R_S t} \qquad (2)$$

t (film thickness) was measured by profilometer.

Synthesis

Synthesis of 3,7-dihydrobenzo[1,2-b:4,5-b']difuran-2,6-dione (BDF)

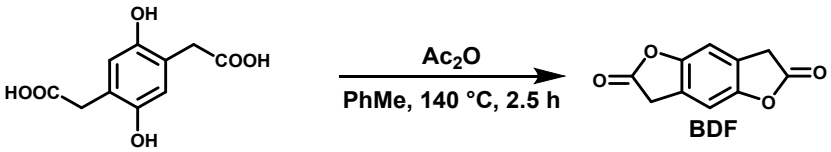

The commercially available 2,2'-(2,5-dihydroxy-1,4-phenylene)diacetic acid (2 g, 8.84 mmol, 1.0 eq.) was suspended in anhydrous toluene (24.0 mL) and acetic anhydride (24.0 mL). The reaction mixture was heated at 140 °C for 2.5 h under N_2 protection. After that, the reaction was cooled to room temperature and BDF precipitates as white crystals. The crystals were filtered and washed with toluene and dried over vacuum (1.34 g, 80%). ^{1}H NMR (500 MHz, DMSO-d_6): δ (ppm) 7.25 (s, 2H), 3.95 (s, 4H); ^{13}C NMR (125 MHz, DMSO-d_6): δ (ppm) 174.3, 150.1, 123.9, 107.3, 33.3.

Synthesis of (*E*)-2H,2'H-[3,3'-bibenzofuranylidene]-2,2'-dione (BFD):

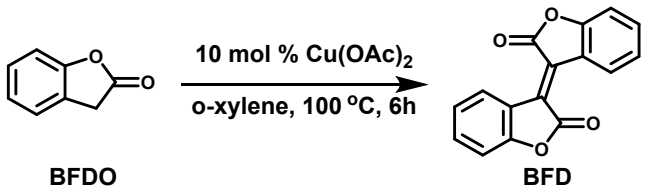

BFD was synthesized via previously reported procedure.[2] In a 100 mL single neck round bottom flask, benzofuran-2(3H)-one (250mg, 1.86 mmol) and $Cu(OAc)_2$ (84.5 mg , 0.46 mmol) were added to *o*-xylene (15 ml) and the mixture was stirred at 100 °C for 6 h. The progress of reaction was checked with TLC, after the

completion of the reaction, the mixture was cooled to room temperature. The reaction mixture was filtered through Celite and washed with DCM. The product was purified via silica-gel column chromatography (hexane:DCM= 1:1 v/v) and then recrystallized using hot hexanes to obtain BFD, which appears as an orange crystalline solid (118 mg, 48%). ^{1}H NMR (400 MHz, $CDCl_3$): δ (ppm) 9.10 (d, 2H), 7.53 (m, 2H), 7.28 (d, 2H), 7.17 (d, 2H); ^{13}C NMR (125 MHz, $CDCl_3$): δ (ppm) 166.9, 156.1, 134.7, 129.88, 129.2, 124.8, 122.6, 110.9.

Synthesis of chromeno[4,3-*c*] chromene-5,11-dione:

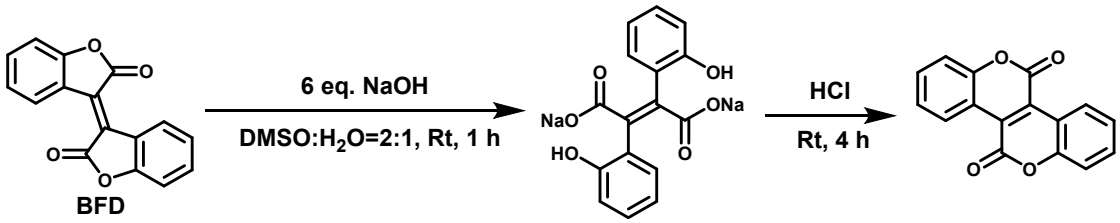

CCD was synthesized via our two-step method of isomerization where alkaline ring-opening hydrolysis followed by acid-mediated ring-closing reaction of BFD leads to the formation of CCD. In a 20 mL vial, (*E*)-2H,2'H-[3,3'-bibenzofuranylidene]-2,2'-dione (BFD) (40mg, 0.135 mmol) was taken. In a separate 20 mL vial, NaOH (32 mg, 0.81 mmol) was dissolved in DMSO/H_2O (2:1 v/v, 10mL). This aqueous NaOH solution was then added to the vial with BFD and stirred at room temperature for 1 h. The progress of the reaction was monitored by the UV-Vis-NIR absorption spectra in DMSO. After the completion of alkaline ring opening hydrolysis reaction, concentrated HCl (1mL) was added to the reaction mixture and stirred for another 4 h to perform acid mediated ring closing reaction. During this reaction, the product CCD precipitates out of the solution. These solids were collected via filtration and were passed through a short silica plug (2:1 DCM/ hexanes) and concentrated to obtain CCD as a yellow solid (14.2 mg, 71% yield). ^{1}H NMR (400 MHz, $CDCl_3$): δ (ppm) 9.26 (d, J = 8 Hz, 2H), 7.64 (m, 2H), 7.45 (m, 4H); ^{13}C NMR (125 MHz, $CDCl_3$): δ (ppm) 158.0, 152.7,132.6, 128.5, 126.6, 125.6, 116.7, 115.8. HRMS (APCI-): calcd. for [$C_{16}H_8O_4$] 264.042; found 264.044.

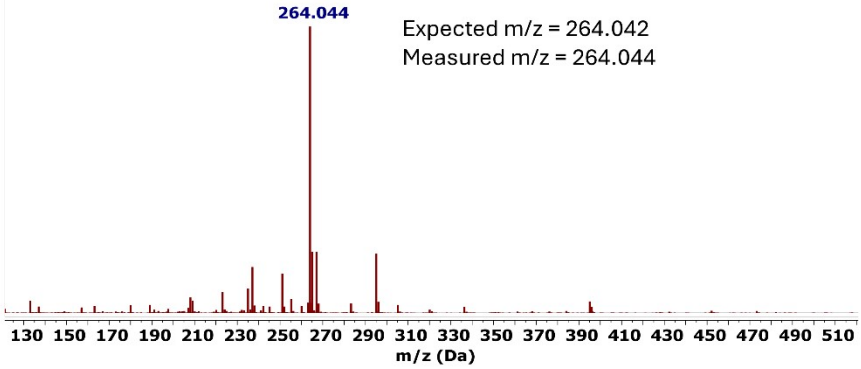

Fig. S1 High resolution mass spectrum of CCD.

Synthesis of 7-(tert-butyl)benzofuran-2,3-dione:

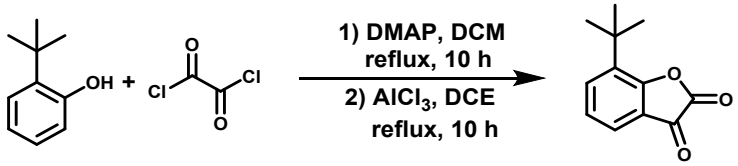

7-(*tert*-butyl)benzofuran-2,3-dione was synthesized via Friedel-Crafts acylation of 2-*tert*-butylphenol. In a 250 mL single neck round bottom flask, 2-*tert*-butylphenol (6.0 g, 39.9 mmol) and 4-(dimethylamino)pyridine (DMAP, 0.48 g, 3.99 mmol) were dissolved in dichloromethane (100 mL). To this solution, oxalyl chloride

(7.45 mL, 87.8 mmol) was added dropwise. The reaction was then refluxed at 45 °C for 10 h and the progress of the reaction was checked with TLC. After the conversion of all the starting material, the solvent was removed via rotary evaporation. After that, the residue was dissolved into 1,2-dichloroethane (50 mL). Aluminum chloride (15.97 g, 119.8 mmol) was added to the solution in three equal portions for 30 min. The reaction mixture was stirred at room temperature for 10 h. Next, the reaction was quenched with ice, extracted with dichloromethane, dried over Na_2SO_4, and followed by rotary evaporation. The residue was recrystallized in hot hexane to obtain pure product as an orange crystalline solid (5.1g, 63% yield). ^{1}H NMR (400 MHz, $CDCl_3$): δ (ppm) 7.72 (dd, *J* = 1.3 Hz, 7.8 Hz, 1H), 7.59 (dd, *J* = 1.3 Hz, 7.5 Hz, 1H), 7.26 (t, *J* = 7.7 Hz, 1H), 1.44 (s, 9H); ^{13}C NMR (125 MHz, $CDCl_3$): δ (ppm) 178.0, 162.3, 155.9, 137.8, 136.9, 125.6, 123.3, 119.5, 34.5, 29.5. Analytical data matches previously reported literature.[3]

Synthesis of 3,7-bis((*E*)-7-(*tert*-butyl)-2-oxobenzofuran-3(2H)-ylidene)-3,7-dihydrobenzo[1,2-b:4,5-b']difuran-2,6-dione (BFD_2):

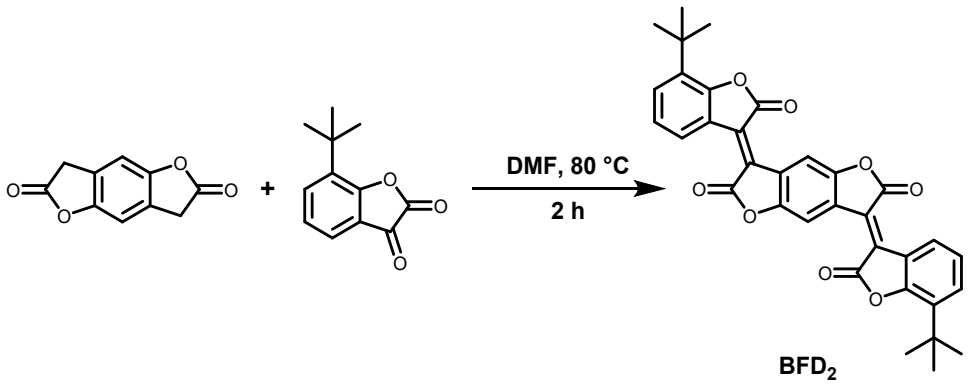

BFD_2 was synthesized via condensation reaction between 3,7-dihydrobenzo[1,2-b:4,5-b']difuran-2,6-dione (BDF) and 7-(*tert*-butyl)benzofuran-2,3-dione, according to a modified literature procedure.[3] In a 20 mL Schlenk tube, 3,7-dihydrobenzo[1,2-*b*:4,5-*b'*]difuran-2,6-dione (0.1 g, 0.52 mmol) and 7-(*tert*-butyl)benzofuran-2,3-dione (0.22 g, 1.09 mmol) was taken, dissolved into DMF (10 mL), and heated at 100 °C for 2 h under an inert atmosphere. The progress of the reaction was monitored by TLC. After the conversion of all BDF, the solvent was removed via rotary evaporation. The residue was dissolved in the minimum amount of dichloromethane and precipitated into hexanes and the solids were collected via filtration. The solids were purified via silica gel column chromatography (2:1 DCM:hexanes) and concentrated. The residue was recrystallized in hot hexanes which yielded a purple solid (114 mg, 39% yield). ^{1}H NMR (400 MHz, $CDCl_3$): δ (ppm) 8.99 (dd, *J* = 0.8 Hz, 6.4 Hz, 2H), 8.93 (s, 2H), 7.54 (dd, *J* = 1.2 Hz, 6.4 Hz, 2H), 7.22 (t, *J* = 6.4 Hz, 2H), 1.46 (s, 18H)); ^{13}C NMR (125 MHz, $CDCl_3$): δ (ppm) 166.6, 166.4, 154.9, 152.3, 134.2, 133.7, 128.0, 127.0, 124.8, 123.1, 110.9, 34.5, 29.7.

Synthesis of CCD_2

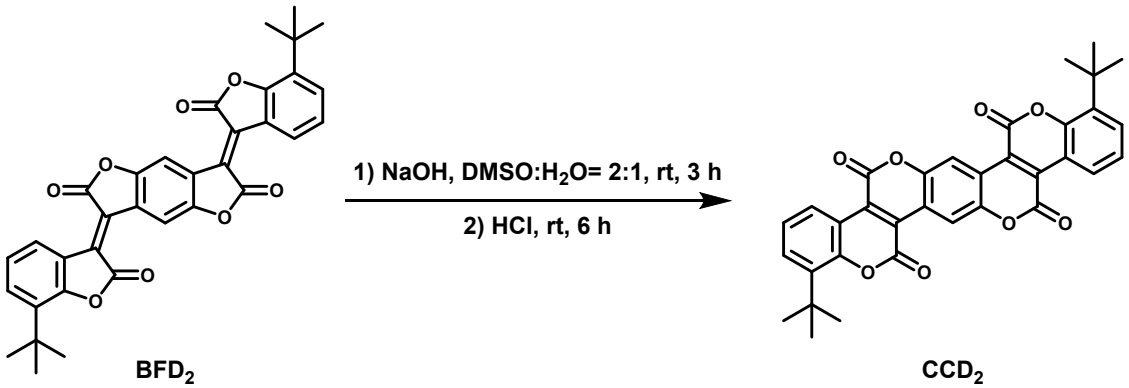

CCD_2 was synthesized via our two-step method of isomerization where alkaline ring-opening hydrolysis followed by acid-mediated ring-closing reaction of BFD_2 leads to the formation of CCD_2. In a 20 mL vial,

BFD_2 (40mg, 0.07 mmol) was taken. In a separate 20 mL vial, NaOH (33.6 mg, 0.84 mmol) was dissolved in DMSO/H_2O (2:1 v/v, 10mL). This aqueous NaOH solution was then added to the vial with BFD_2 and stirred at room temperature for 3 h. The progress of the reaction was monitored by UV-Vis-NIR absorption spectra in DMSO. After the completion of the alkaline ring opening hydrolysis reaction, concentrated HCl (1mL) was added to the reaction mixture and stirred for another 6 h to perform acid mediated ring closing reaction. During this reaction, the product CCD_2 precipitated out of the solution and was collected via filtration. The residue was dissolved in a minimum amount of dichloromethane and precipitated into hexanes and then, the solids were again collected via filtration. The solids were then purified via silica gel column chromatography (2:1 DCM:hexanes) and concentrated to yield an orange solid (30.4 mg, 76% yield). ^{1}H NMR (500 MHz, $CDCl_3$): δ (ppm) 9.36 (s, 2H), 9.18 (d, J = 8 Hz, 2H), 7.71 (d, J = 7.5 Hz, 2H), 7.41 (t, J = 6.4 Hz, 8H), 1.58 (s, 18H); ^{13}C NMR (125 MHz, $CDCl_3$): δ (ppm) 157.4, 157.2, 152.2, 149.0, 137.9, 131.4, 129.4, 126.9, 125.4, 124.0, 118.6, 116.1, 115.4, 35.3, 30.1. HRMS (APCI-): calcd. for $[C_{34}H_{26}O_8]^-$: m/z = 562.1628, found: m/z = 562.1640.

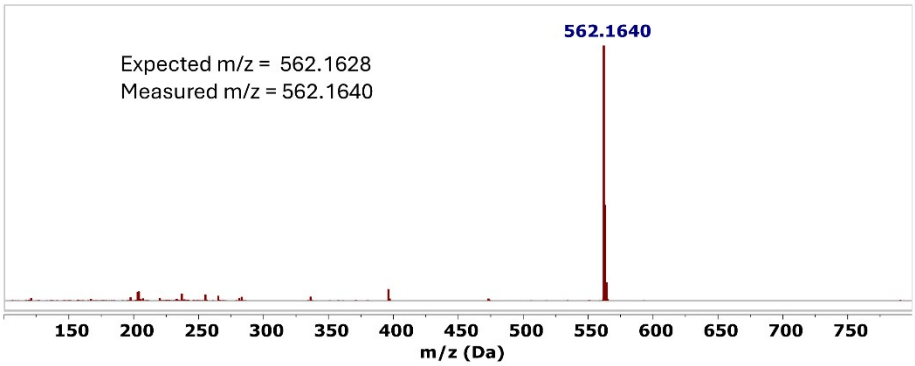

Fig. S2 High resolution mass spectrum of CCD_2.

Synthesis of n-doped poly(benzodifurandione) (n-PBDF):

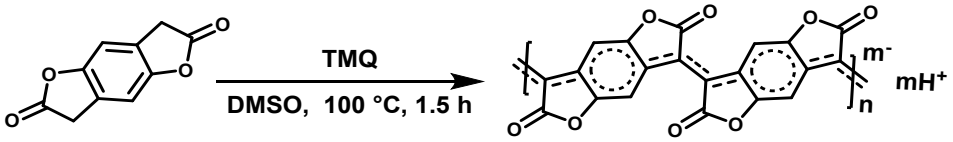

BDF n-PBDF

n-Doped poly(benzodifurandione) (n-PBDF) was synthesized with slight modifications according to a previously reported procedure.[4] BDF monomer (600 mg, 3.15 mmol) and TMQ (1,034 mg, 6.30 mmol) were charged into a 100 mL two-neck round-bottom flask equipped with a magnetic stir bar. The flask was evacuated and backfilled with nitrogen five times to ensure an inert atmosphere. Anhydrous extra-dry DMSO (20 mL, 99.9%) was added under nitrogen, and the flask was further evacuated and backfilled with nitrogen three additional times at room temperature. The reaction mixture was stirred vigorously at 100 °C for 1.5 h, during which the solution color changed from yellow to dark black with a significant increase in viscosity. After cooling to room temperature, additional DMSO (10 mL) was added to reduce viscosity. The resulting solution was transferred to a dialysis membrane (MWCO = 10 kDa) and dialyzed against DMSO for 4 days, with the external solvent replaced every 12 h to remove low-molecular-weight species. The purified polymer solution was collected from the dialysis bag. Removal of unreacted monomer was confirmed by ^{1}H NMR spectroscopy (300 μL polymer solution dissolved in 300 μL DMSO-d_6). The polymer concentration was determined gravimetrically by drying 2 mL of the polymer solution in a pre-weighed 20 mL glass vial under vacuum at 70 °C for 12 h.

Detailed synthesis of Poly(chromenochromenedione) (PCCD):

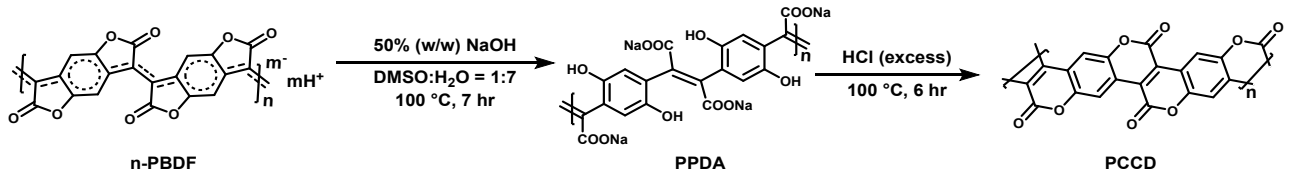

In a 250 mL two-neck round bottom flask, 20 mL of n-PBDF (8 mg/ml, in DMSO) was taken under a nitrogen environment. Separately, NaOH (80 mg, 50 wt% n-PBDF) was dissolved in deionized water (140 mL) in a 250 mL beaker. The aq. NaOH was added to the n-PBDF solution, and the reaction mixture was heated to 100 °C and stirred for 7 h. The progress of the reaction was monitored by UV-Vis-NIR absorption spectroscopy. Completion of the reaction was indicated by the disappearance of characteristic polaron and bipolaron absorption of n-PBDF in the NIR region and the appearance of a new peak at 377 nm that is characteristic of PPDA. This confirms the completion of lactone ring-opening hydrolysis reaction along the n-PBDF polymer chains. During this process, the reaction color changed from black to yellow. Subsequently, concentrated HCl (40 ml) was then added to the reaction mixture and stirred at 100 °C for an additional 6 h to induce acid mediated six-member lactonization reaction affording PCCD polymer. PCCD is insoluble in the reaction mixture and precipitates immediately after the ring closing reaction. After cooling to room temperature, the supernatant was decanted, and the heterogeneous PCCD/water phase was transferred to centrifuge tubes. The reaction mixture was cooled down to room temperature, and the supernatant was decanted, and the PCCD/water heterogeneous mixture was transferred to centrifuge tubes. The solid was collected by centrifugation (4000 rpm, 10min), the acidic supernatant was removed, and the residue was washed with deionized water three times using centrifugation followed by decantation. The resulting dark pink slurry was filtered through a nylon membrane (pore size, 10μm) and washed with MeOH to remove residual water and DMSO. The obtained pink solid was dried under vacuum to yield PCCD as a dark pink solid (134 mg, 84%). To obtain the UV-vis absorption spectra, a 0.1 mg/ml dispersion was created in DMSO by ultrasonication for 30 min, which was diluted further with DMSO to make a solution of 0.05 mM concentration. This was ultrasonicated for another 30 min before obtaining the absorbance spectra in DMSO. For the thin film absorbance spectra of PCCD, the 0.1 mg/ml dispersion of PCCD in DMSO was drop casted on a 1 cm × 1 cm precleaned and UV-Ozone treated glass substrate, then dried in a vacuum oven for 1 hour to ensure complete solvent removal before obtaining the thin film absorbance spectra.

Detailed synthesis of n-doped Poly(chromenochromenedione) (n-PCCD N-DMBI$^+$):

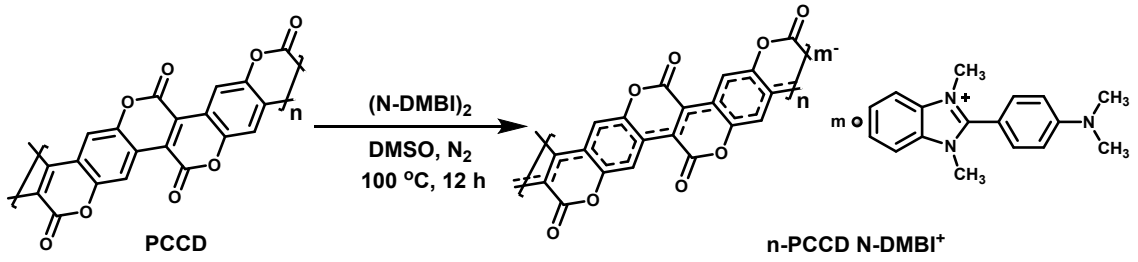

$(N\text{-}DMBI)_2$ was synthesized according to a previously reported procedure.[5] PCCD (16 mg) was taken in a 20 mL vial under nitrogen protection. $(N\text{-}DMBI)_2$ (8mg, 50 wt%) was added to the vial with PCCD. 2 ml of anhydrous DMSO was added to the solid mixture to maintain PCCD concentration (8mg/ml). The vial was sealed and ultrasonicated for 30 min followed by heating at 100 °C for 12 hr. The UV-Vis-NIR absorption spectra of the doped polymer inks were obtained in DMSO (0.07 mM) which showed a lowering of neutral polymer absorbance with a rise of polaron absorbance in the NIR region.

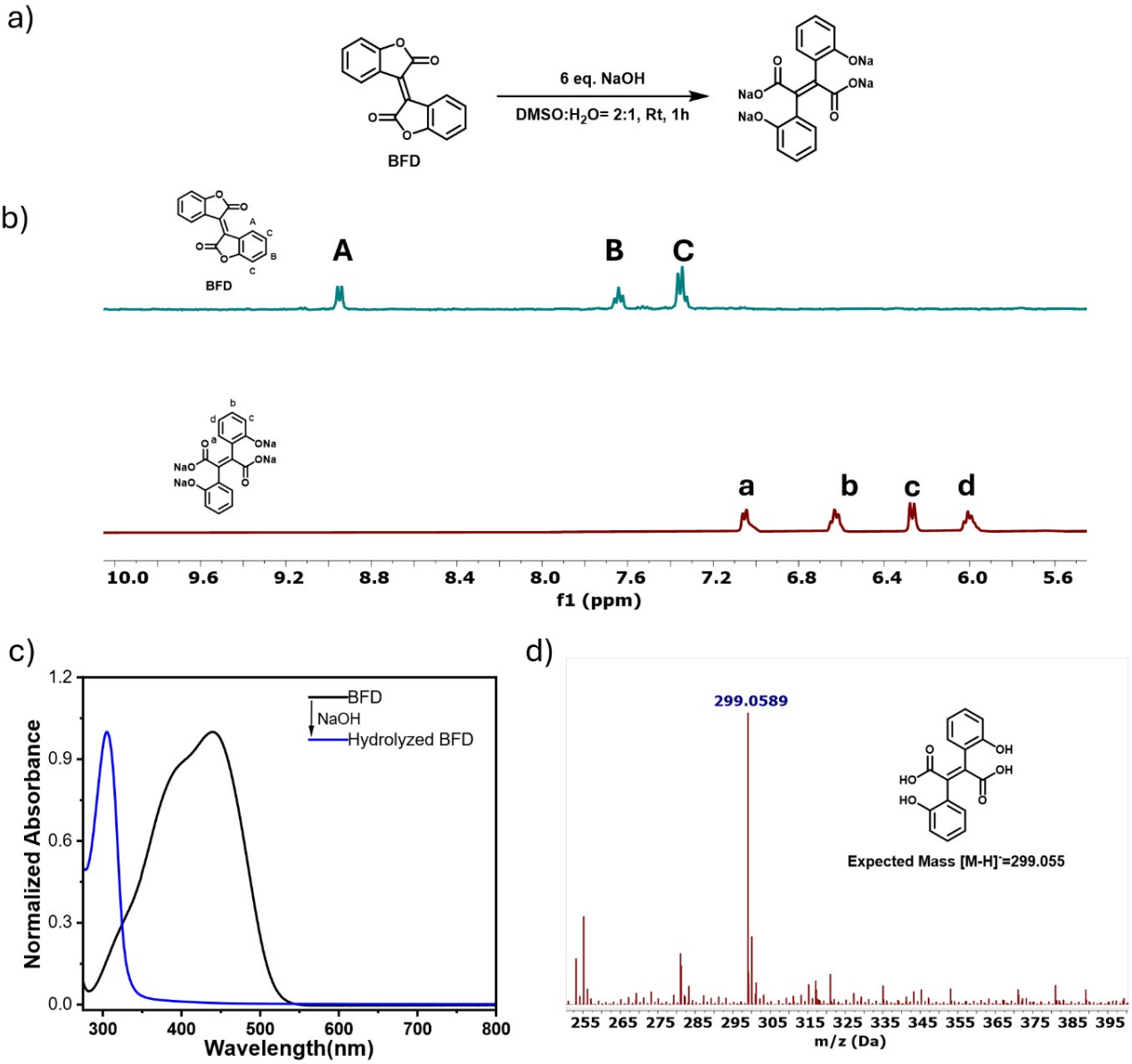

Fig. S3 a) Schematic illustration for BFD hydrolysis, b) stacked ^{1}H NMR of BFD and in situ ^{1}H NMR of reaction mixture after hydrolysis in DMSO-d_6, c) UV-Vis absorption spectra of BFD and hydrolyzed BFD in DMSO, and d) negative mode ESI-MS of BFD ring opening hydrolysis mixture after hydrolysis.

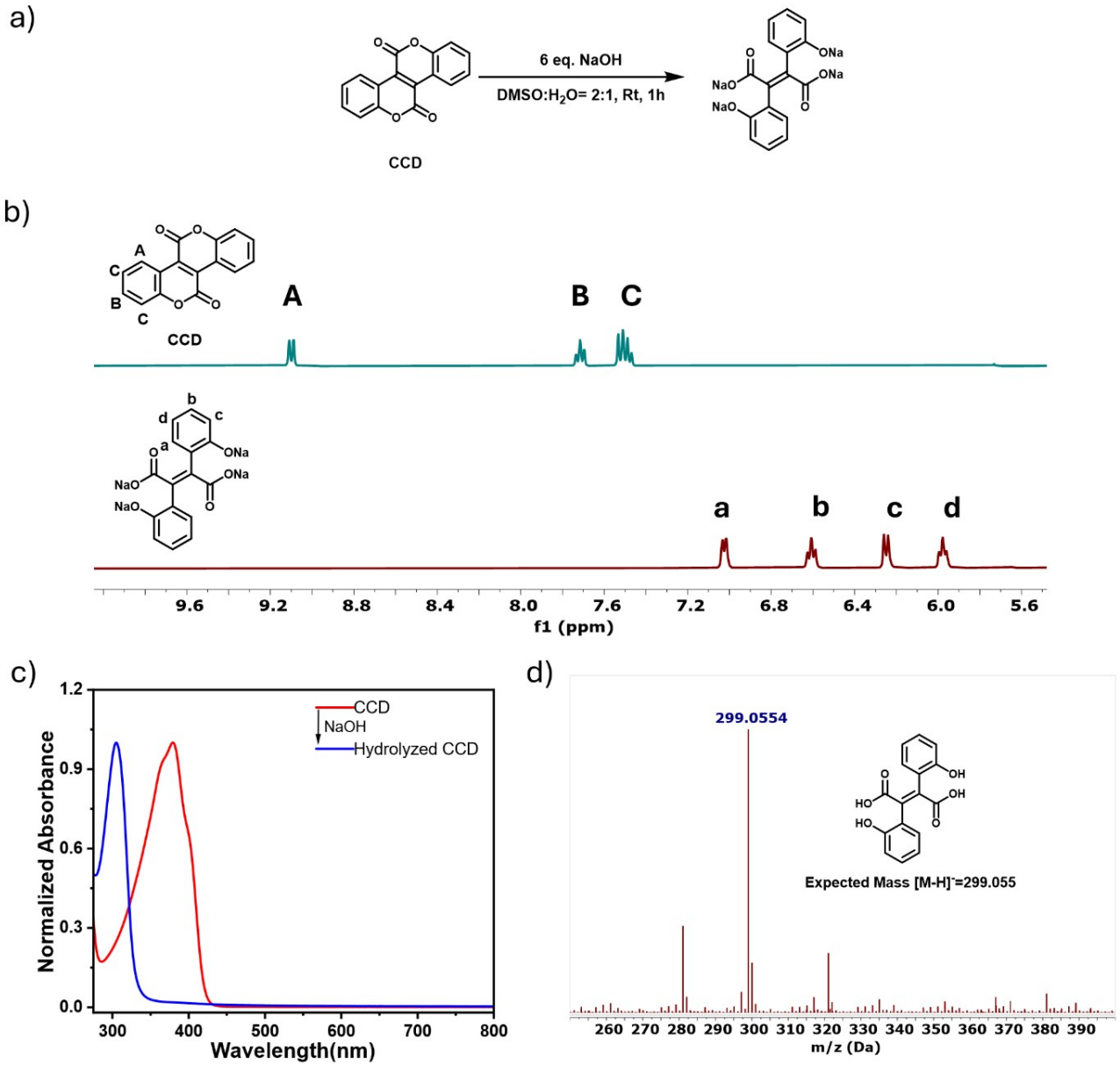

Fig. S4 a) Schematic illustration for CCD hydrolysis, b) stacked ^{1}H NMR of CCD and in situ ^{1}H NMR of reaction mixture after hydrolysis in DMSO-d_6, c) UV-Vis absorption spectra of CCD and hydrolyzed CCD in DMSO, and d) negative mode ESI-MS of CCD ring-opening hydrolysis mixture after hydrolysis.

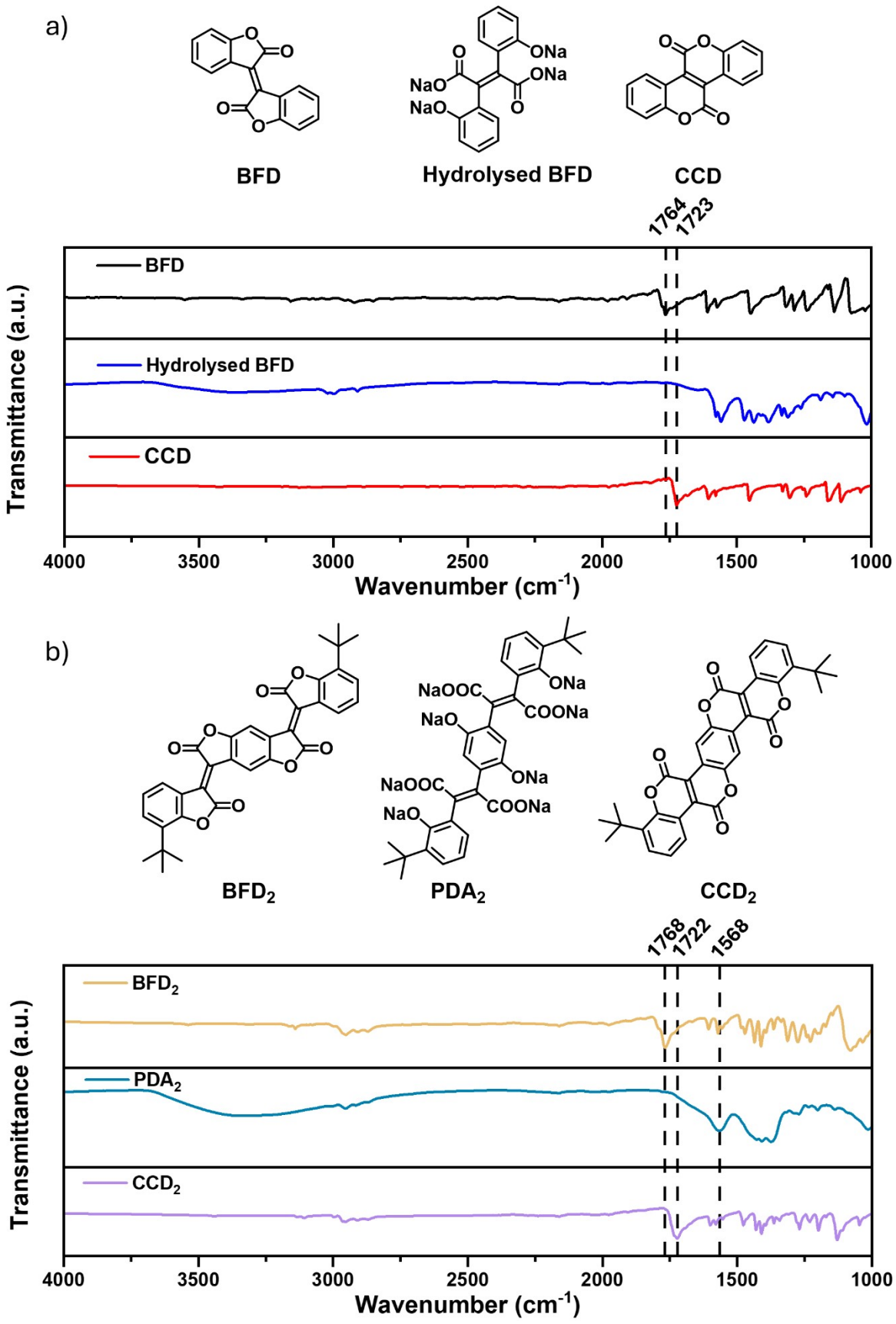

Fig. S5 Chemical structure and corresponding stacked full FTIR spectra a) BFD, hydrolyzed BFD, and CCD b) BFD_2, PDA_2, and CCD_2.

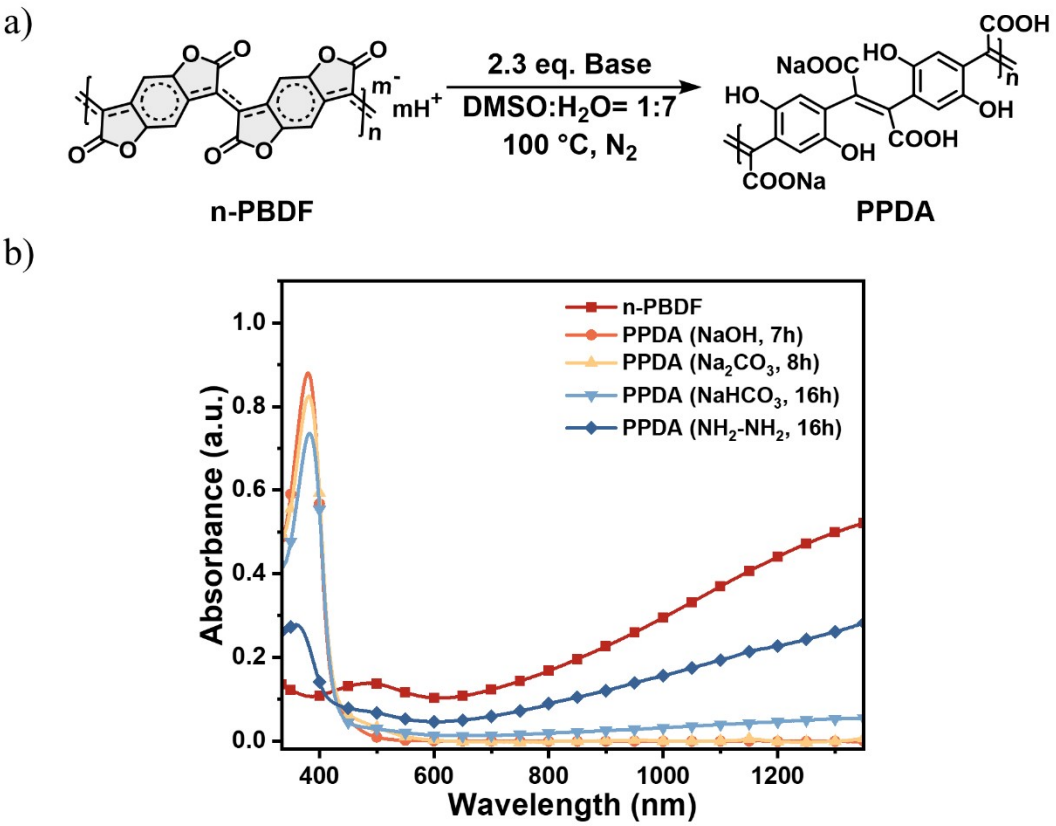

Fig. S6 Base-dependent ring-opening hydrolysis of n-PBDF to PPDA. a) Schematic illustration of the ring opening hydrolysis n-PBDF to PPDA with the same molar equivalents of different bases. b) UV-Vis-NIR absorption spectra of the reaction mixtures in water after hydrolysis. NaOH and Na_2CO_3 led to a complete disappearance of n-PBDF NIR absorption and formation of PPDA absorption band at 377 nm. However, $NaHCO_3$ and NH_2NH_2 resulted only in partial conversion, indicating incomplete ring opening hydrolysis.

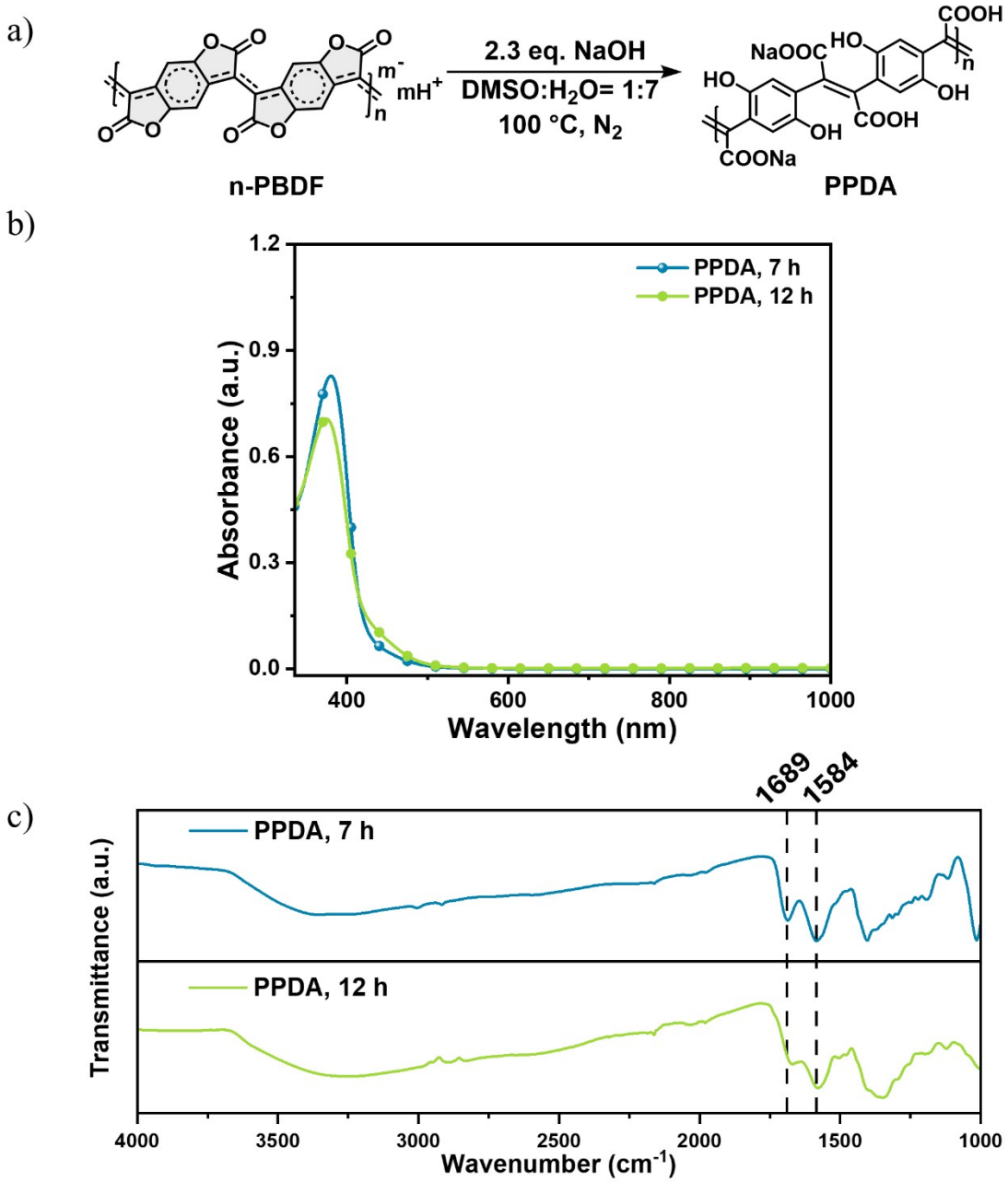

Fig. S7 Stability of PPDA under alkaline hydrolysis conditions. The reaction mixture was heated for an additional 5 h after completion of n-PBDF hydrolysis to assess the stability of PPDA. a) Schematic illustration of the n-PBDF hydrolysis with NaOH, b) UV-Vis-NIR absorption spectra of PPDA in water, and c) stacked FTIR spectra of PPDA. The PPDA spectral features remained unchanged after prolonged heating, indicating that PPDA is stable to the alkaline hydrolysis conditions.

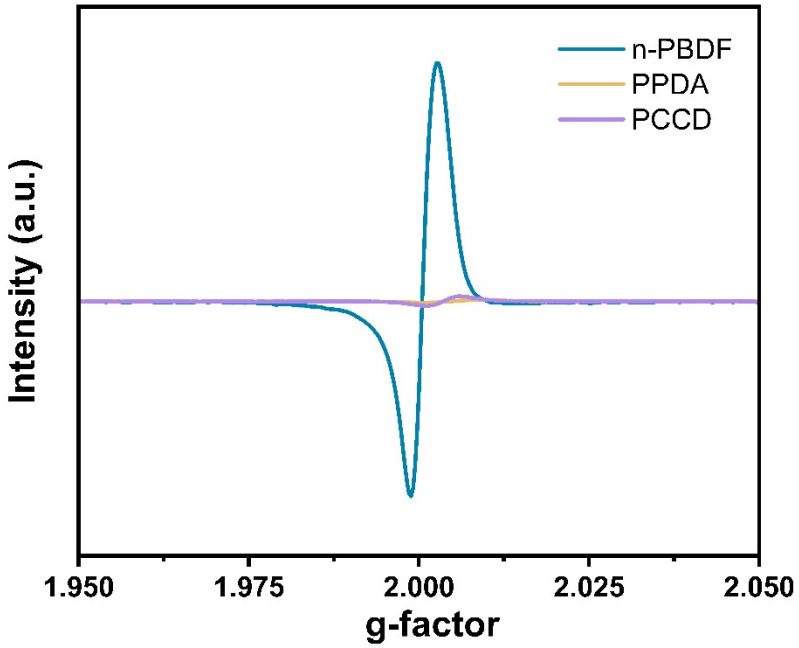

Fig. S8 Overlapping EPR spectra of n-PBDF, PPDA, and PCCD.

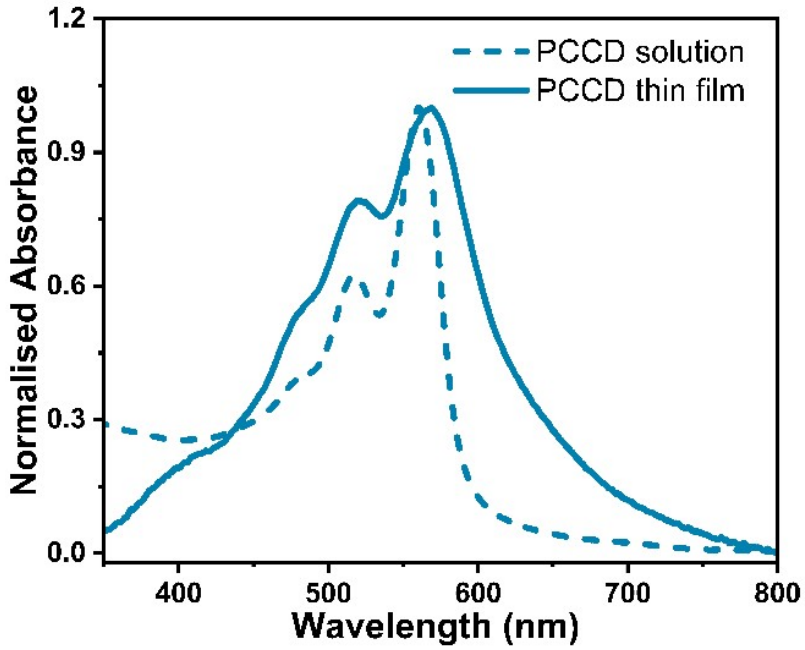

Fig. S9 UV-Vis absorption spectra of PCCD in solution (DMSO) and thin film state.

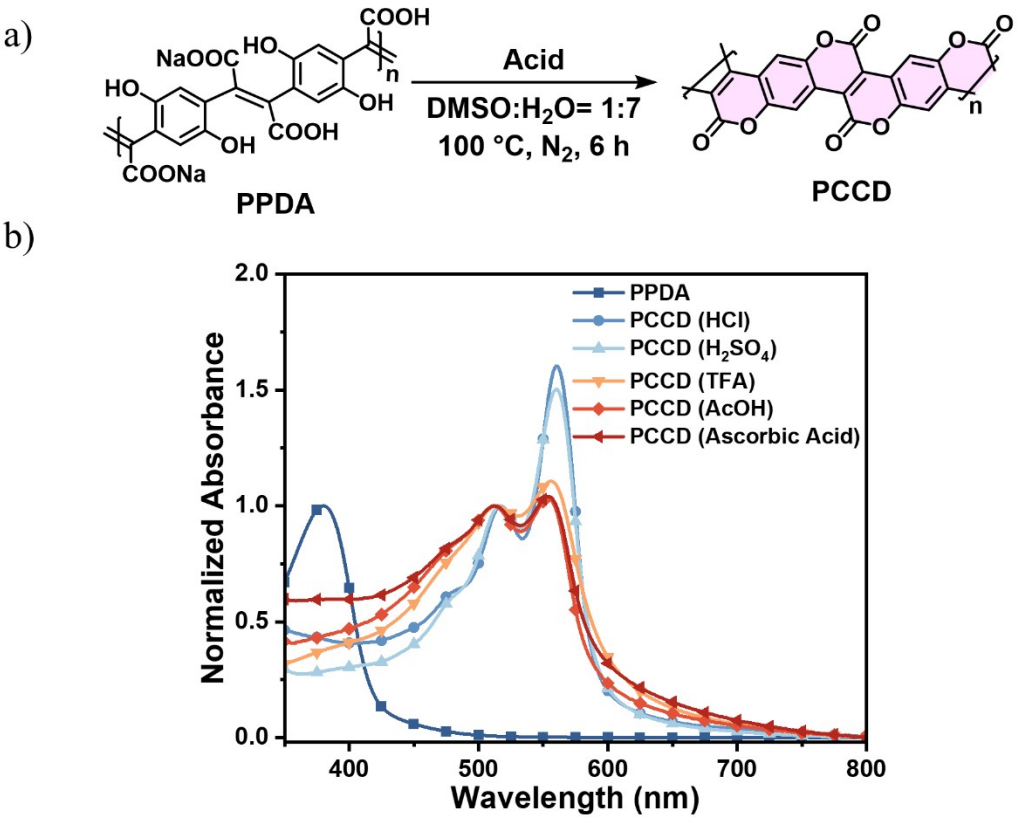

Fig. S10 Acid dependent ring closing of PPDA to PCCD. a) Schematic illustration of the PPDA ring closing reaction to PCCD using the same molar equivalents of different acids. b) UV-Vis absorption spectra of isolated PCCD samples in DMSO obtained from different acid mediated ring closing reactions. The spectra were normalized to the 0-1 transition band of PCCD at 517 nm. Among the acids tested, HCl produced PCCD with the highest relative 0-0 transition band intensity at 560 nm, suggesting enhanced backbone ordering/aggregation in solution, which suggests more efficient ring closing to the rigid PCCD structure.

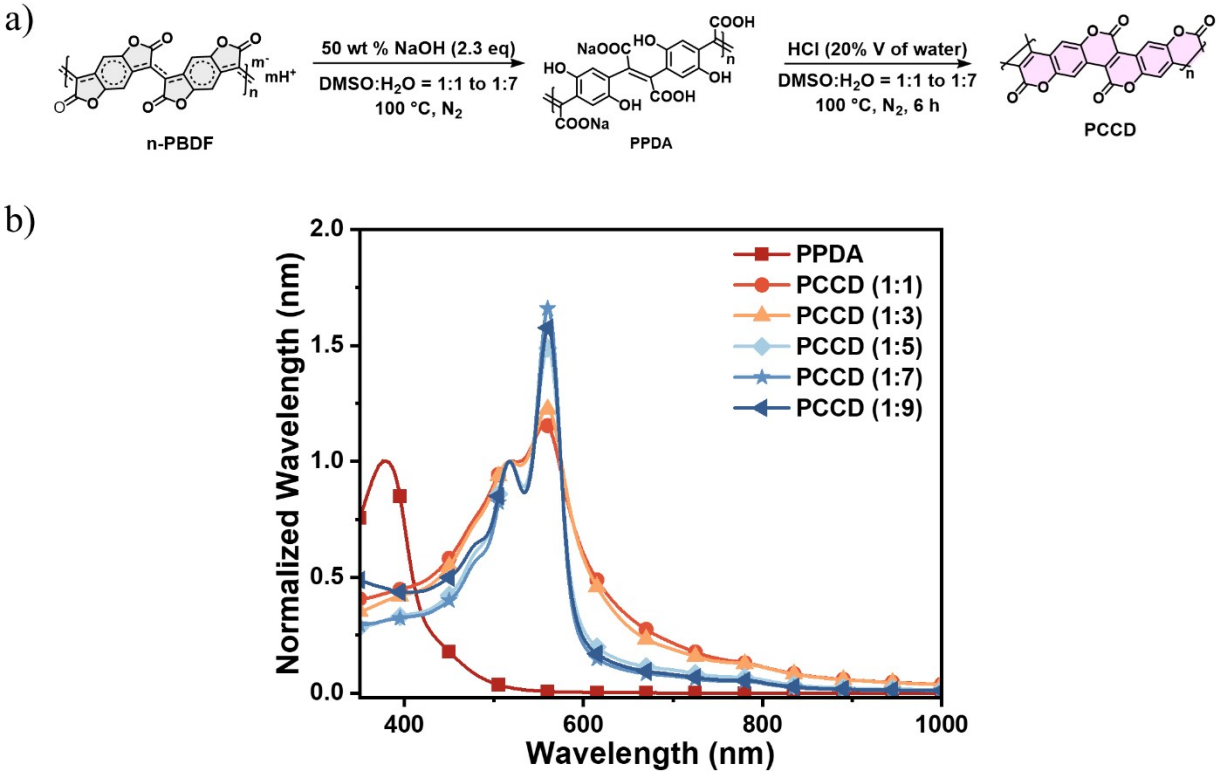

Fig. S11 Effect of DMSO/H_2O ratio on the two-step isomerization of n-PBDF to PCCD. a) Schematic

illustration of the two-step isomerization of n-PBDF to PCCD using different DMSO/H_2O ratios from 1:1 to 1:7, and b) Normalized UV–Vis–NIR absorption spectra of isolated PCCD samples in DMSO. The spectra were normalized to the 0-1 transition band of PCCD at 517 nm. The PCCD sample synthesized using a DMSO/H_2O ratio of 1:7 showed the highest relative 0-0 transition intensity at 560 nm, suggesting enhanced backbone ordering/aggregation. This phenomenon is consistent with improved solubilization of the PPDA intermediate polymer in the water rich solution, enabling more effective acid mediated ring closing and precipitation of PCCD.

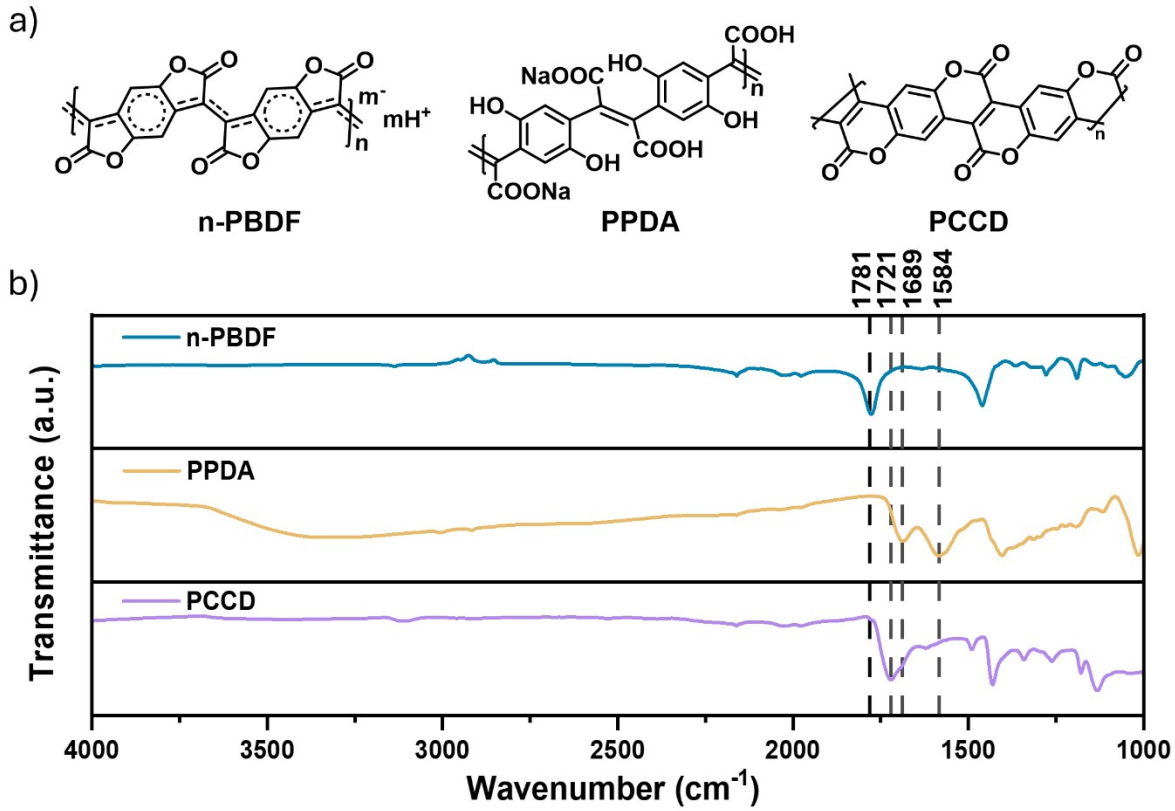

Fig. S12 a) Chemical structures of n-PBDF, PPDA, PCCD, and b) stacked full FTIR spectra of n-PBDF, PPDA, and PCCD.

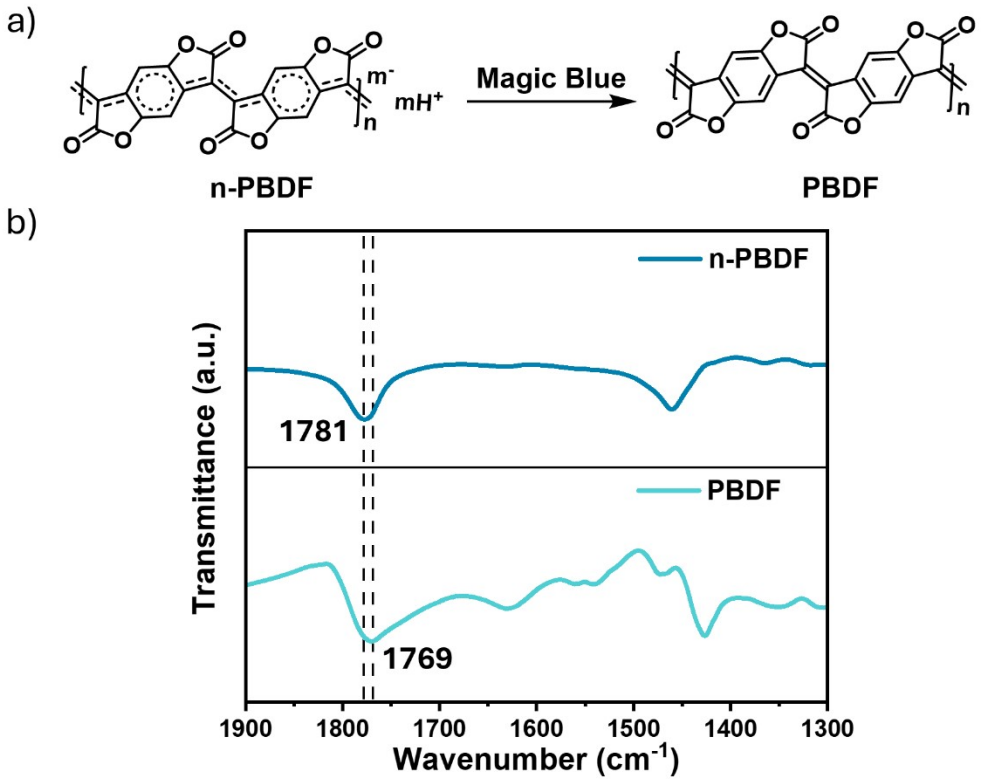

Fig. S13 a) Schematic illustration of the chemical de-doping of n-PBDF thin film to neutral PBDF thin film,[6] and b) Stacked FT-IR spectra of n-PBDF and PBDF.

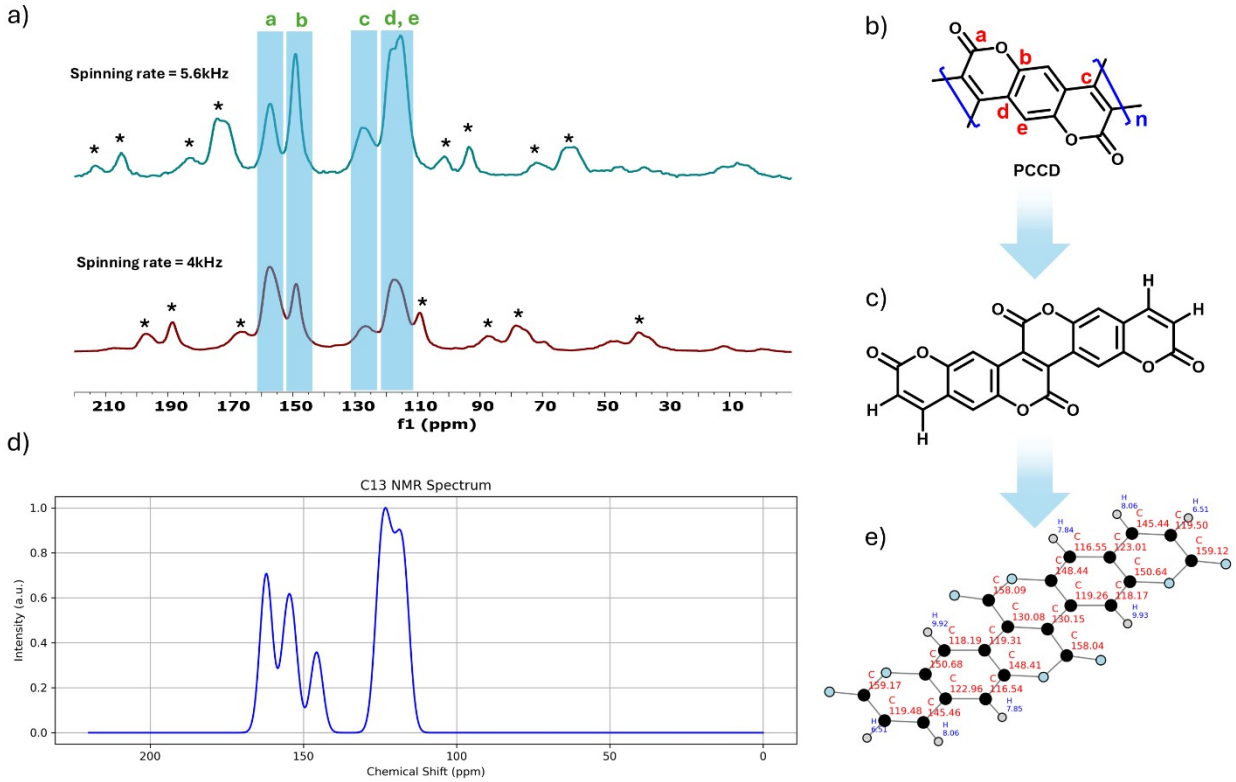

Fig. S14 a) Solid-state ^{13}C CP-MAS NMR spectroscopy of PCCD powder under different spinning rates. Spinning side bands (signals with asterisk sign) appear at ±56 ppm and ±40 ppm from main peaks when the spinning rates are 5.6 kHz and 4 kHz respectively. The true isotropic peaks from PCCD polymer did not shift when spinning rates were changed. However, the spinning sidebands marked as star signs appear at different positions as the spinning rate is varied. b) Chemical structure of PCCD with peak assignment, c) chemical structure of PCCD repeating unit, d) calculated ^{13}C NMR spectrum of PCCD repeating unit, and e) chemical

shifts of PCCD repeating unit. The calculations were done under B3LYP D3BJ 6-311G(d,p) Optimization and wB97X-D4 def2-SVP NMR calculation with chloroform.

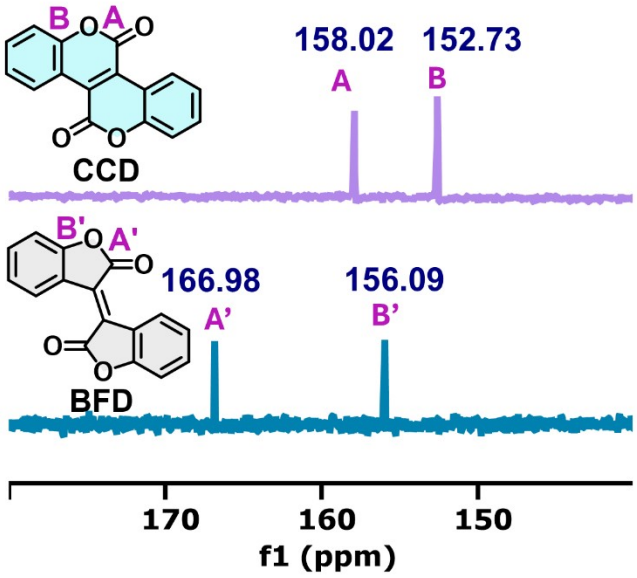

Fig. S15 Stacked ^{13}C NMR spectrum of CCD and BFD in $CDCl_3$ showing the characteristic carbonyl assignments.

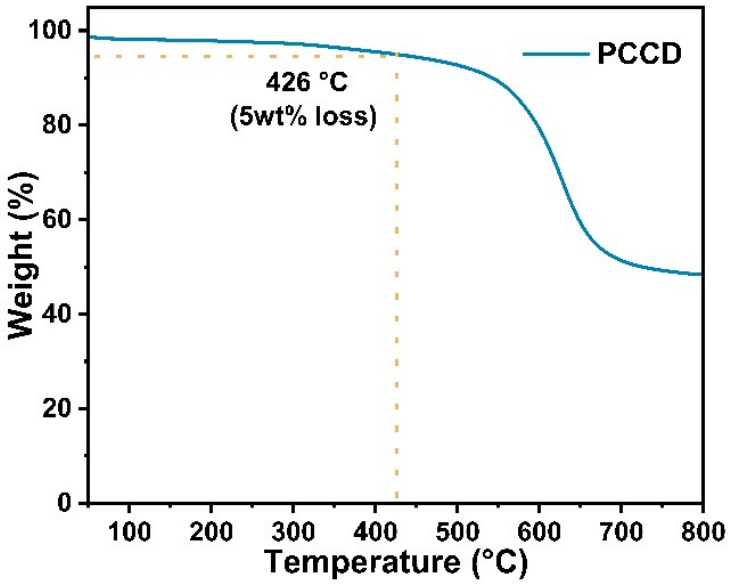

Fig. S16 Thermogravimetric analysis (TGA) of PCCD. PCCD loses 5% weight at 426 °C.

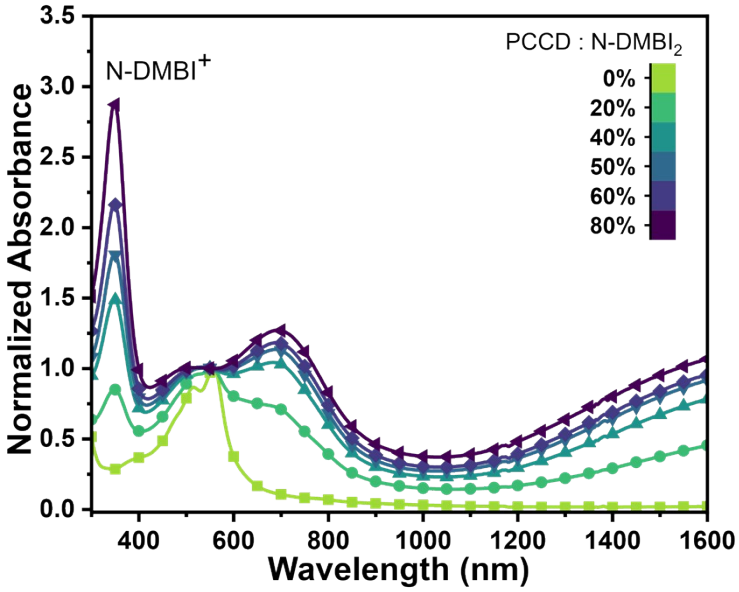

Fig. S17 Full UV-Vis-NIR spectra of n-PCCD inks in DMSO. The strong absorbance at 348 nm is from the $N\text{-}DMBI^+$ countercation which shows a rise in intensity with the increase of wt% of $(N\text{-}DMBI)_2$ dopant.

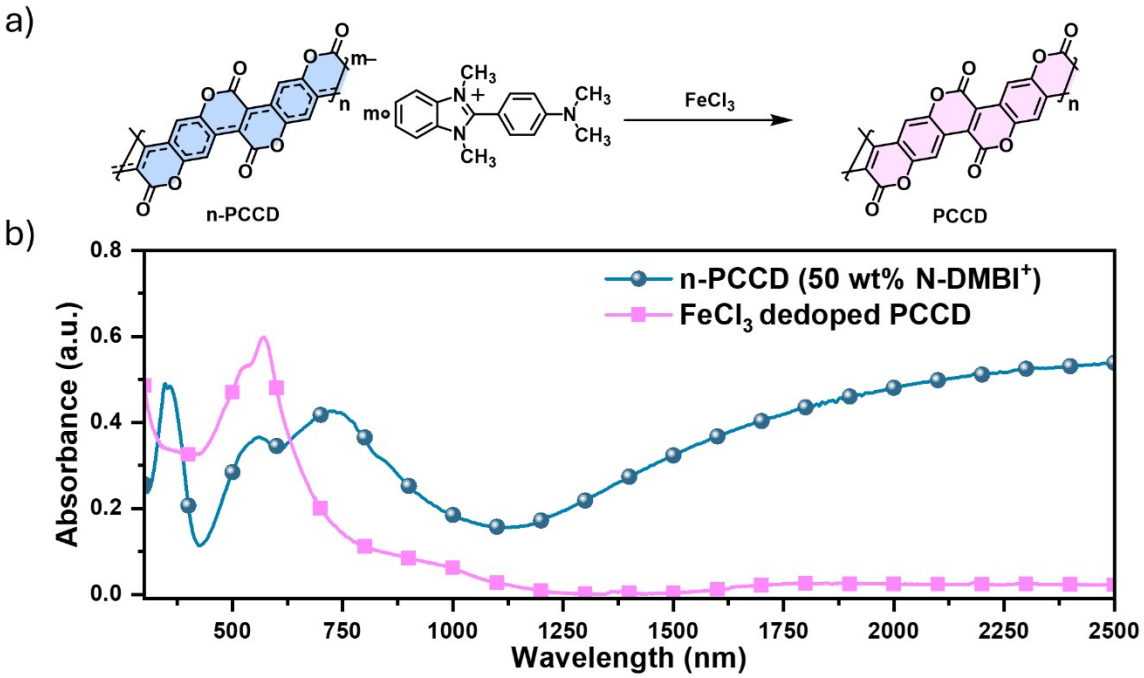

Fig. S18 a) Schematic illustration of the chemical dedoping of n-PCCD (50 wt% $N\text{-}DMBI^+$) thin film to neutral PCCD thin film using $FeCl_3$ acetonitrile solution (10 mM), and b) UV-Vis-NIR absorption spectra of n-PCCD thin film and $FeCl_3$ treated n-PCCD thin films.

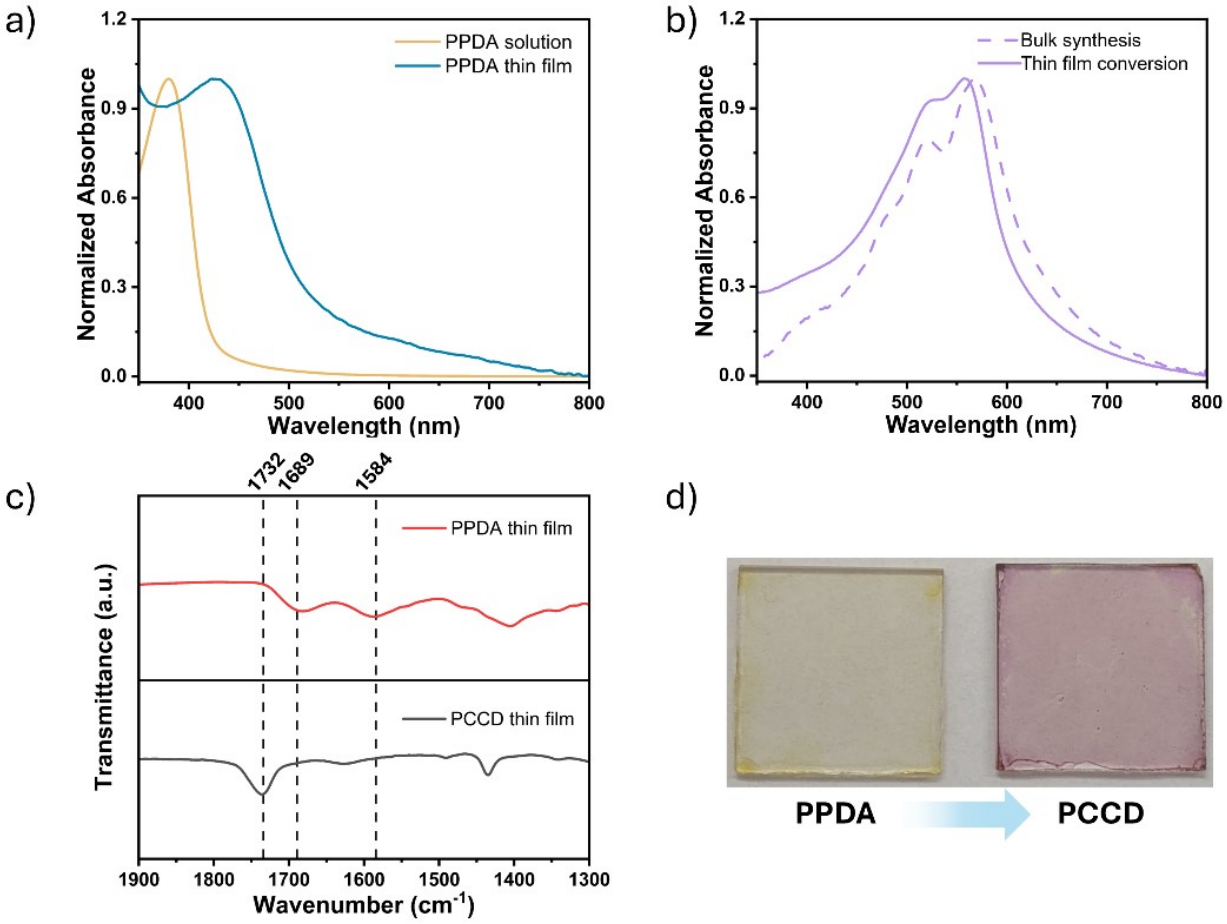

Fig. S19 a) UV-Vis absorption spectra of PPDA in solution (water) and thin film state, b) UV-Vis absorption spectra of PCCD thin films synthesized in bulk solution and in-situ thin film conversion, c) stacked FTIR spectra of PPDA thin films as cast, PCCD (PPDA thin film acidified followed by heating), and d) picture of PPDA (pale yellow) and in-situ converted PCCD (pink) thin films.

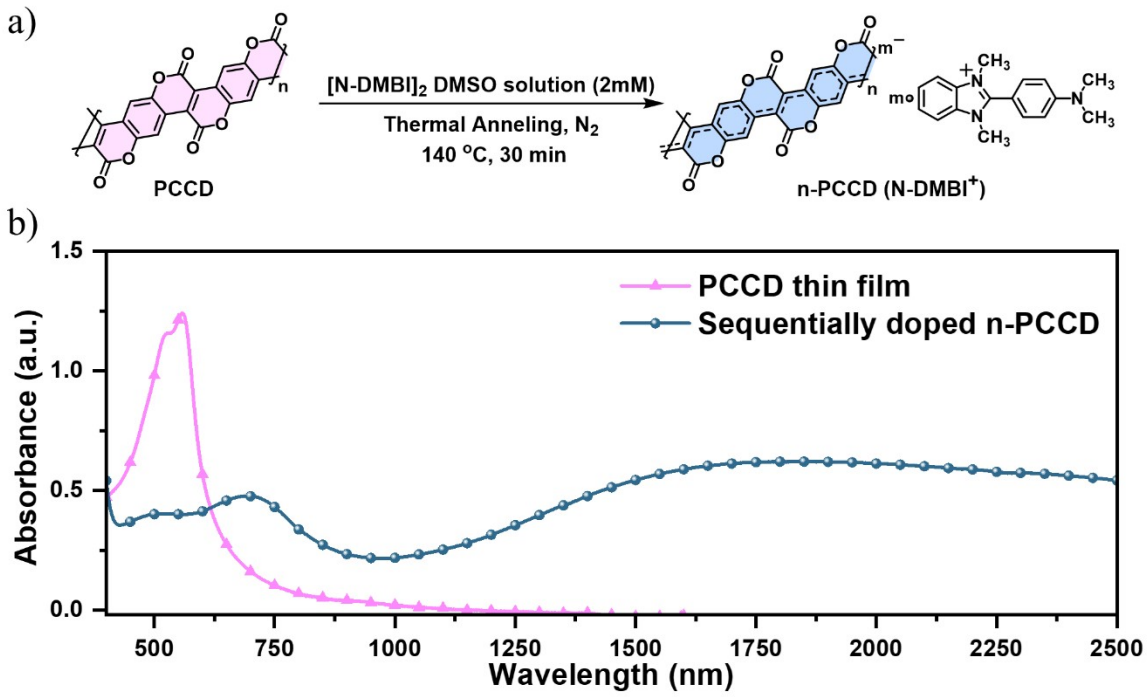

Fig. S20 a) Schematic illustration of the sequential doping of in situ converted PCCD to n-PCCD, and b) UV-Vis-NIR spectra of in situ converted PCCD and sequentially doped PCCD. The rise of NIR absorption

after sequential doping confirms successful formation of the doped n-PCCD state.

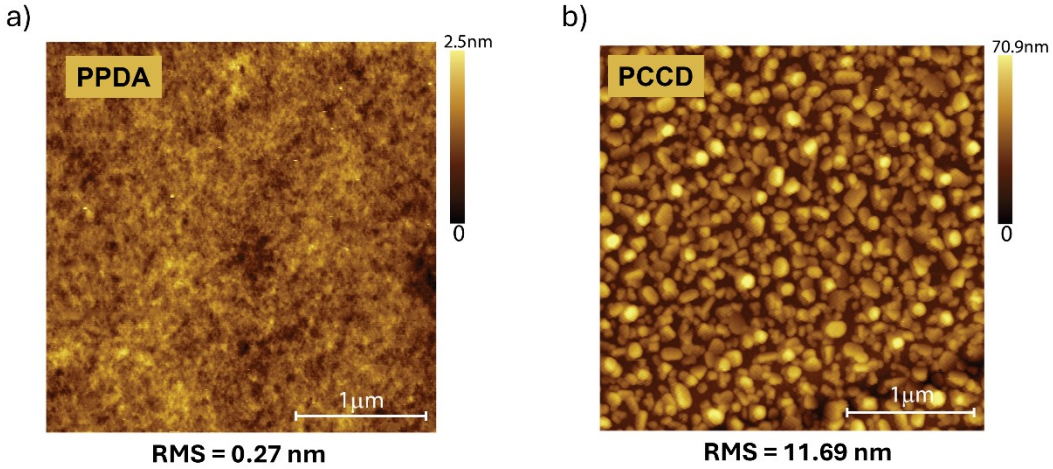

Fig. S21 AFM surface topography image of a) PPDA, and b) PCCD. The smoother morphology of PPDA can be attributed to its polar functional groups and more flexible backbone, which makes it highly soluble in water and suppress interchain packing. However, during the in situ conversion of PPDA to PCCD, a rigid planar PCCD backbone is formed. The increased backbone planarity and rigidity of PCCD promotes stronger interchain π-π interaction and interchain aggregation especially the absence of side chains leads to higher RMS roughness for PCCD thin films.[7]

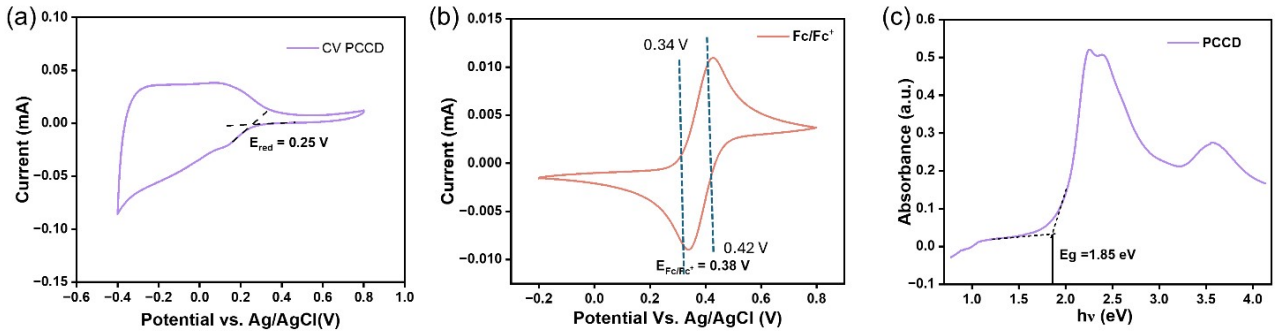

Fig. S22 (a) Cyclic voltammogram (CV) of PCCD recorded at 40 mV/s in 0.2 M TBA-TFSI/PC, showing the onset reduction potential near 0.25 V vs. Ag/AgCl, and (b) CV of ferrocene under identical electrolyte conditions, used as an internal reference ($E_{ox} = 0.42\,V$, $E_{red} = 0.34\,V$). (c) Tauc plot of PCCD.

The LUMO of PCCD was calculated around 4.67 eV consistent with the previously reported value (-4.51 eV)[2] using the following Equation 3:

$$E_{LUMO} = -\left[E_{red} + \left(4.8 - E_{Fc/Fc+}\right)\right] eV \quad (3)$$

$$E_{LUMO} = -[0.25 + (4.8 - 0.38)] eV$$

$$E_{LUMO} = -4.67\ eV$$

Table S1 Crystal data and structure refinement for CCD_2.

Crystal Data	
CCDC number	2539281
Empirical formula	$C_{34}H_{26}O_8$
Formula weight	562.55
Temperature [K]	150
Crystal system	Triclinic, $P\bar{1}$
a, b, c [Å]	6.7456(7), 10.5361(11), 19.3370(18)
α, β, γ [°]	76.704(4), 81.939(5), 85.572(7)
Volume [Å^3]	1322.8(2)
Z	2
μ [mm^{-1}]	0.832
Crystal size [mm^3]	0.450×0.110×0.040
Radiation	CuK_α (λ=1.54178 Å)
Data Collection	
Diffractometer	Bruker AXS D8 Quest four circle diffractometer
Absorption Correction	multi-scan
T_{min}, T_{max}	0.61, 0.754
No. of measured, independent, and observed [$I>2\sigma(I)$] reflections	42376, 5771, 5266
R_{int}	0.0824
Refinement	
$R[F^2> 2\sigma(F^2)]$, $wR(F^2)$, S	0.0479, 0.1498, 1.053
No. of reflections	5771
No. of Parameters	386
No. of Restraints	0
$\Delta\rho_{max}$, $\Delta\rho_{min}$ [eÅ^{-3}]	0.19, −0.23

^{1}H NMR and ^{13}C NMR spectra

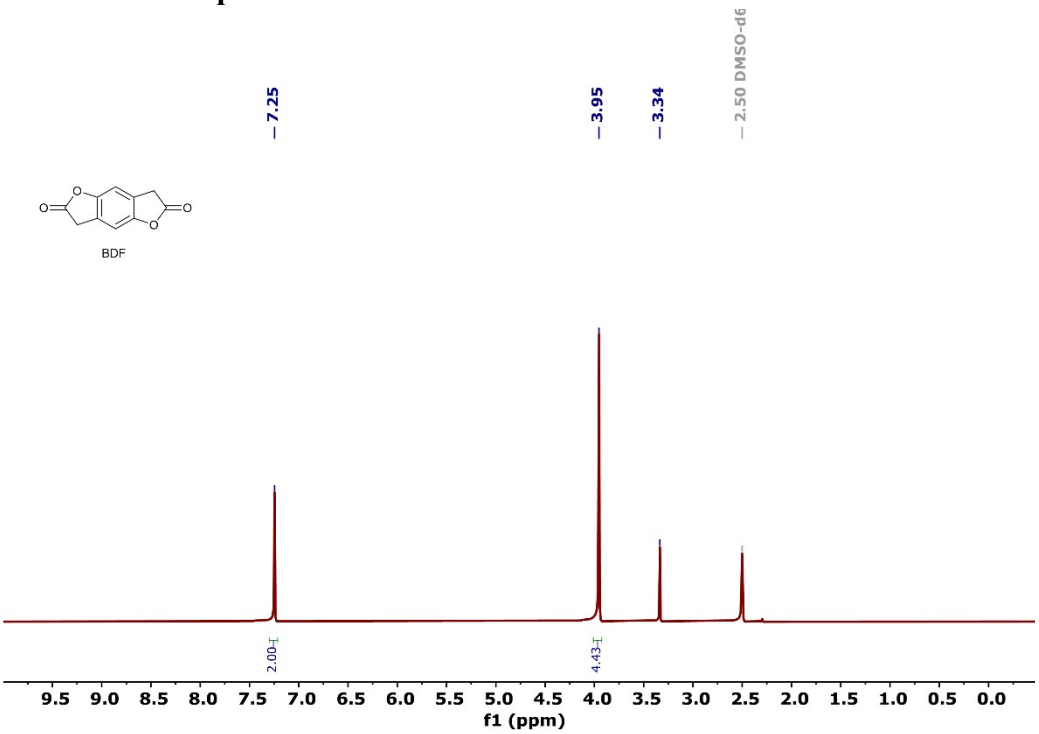

Fig. S23 ^{1}H NMR of 3,7-dihydrobenzo[1,2-b:4,5-b']difuran-2,6-dione.

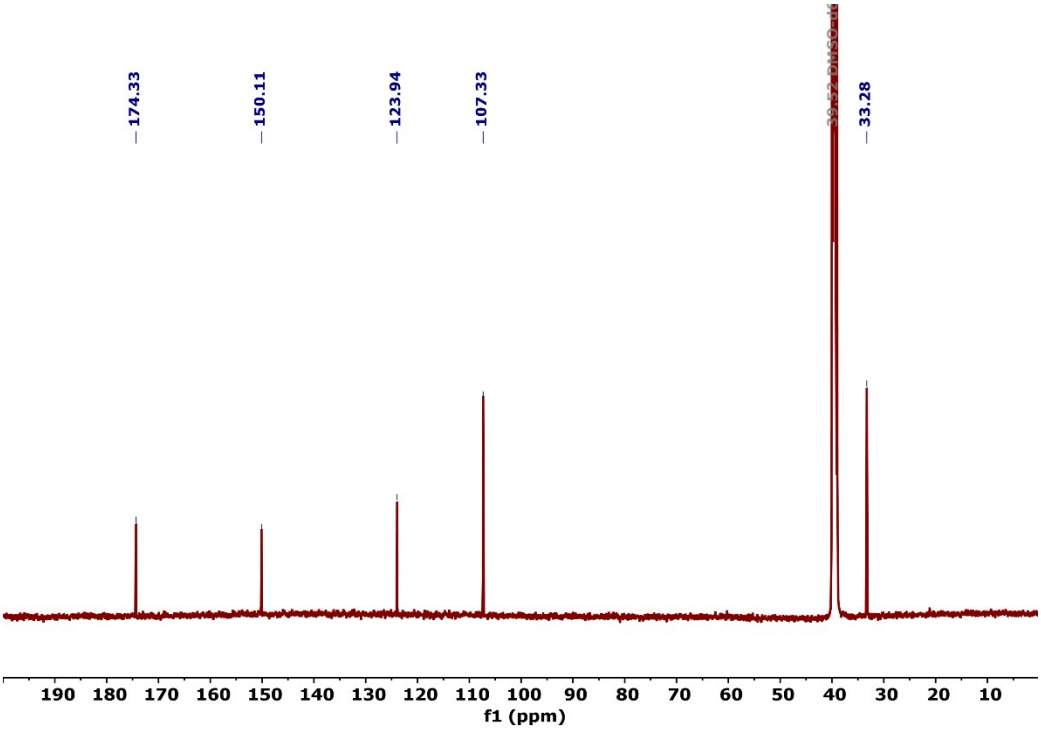

Fig. S24 ^{13}C NMR of 3,7-dihydrobenzo[1,2-b:4,5-b']difuran-2,6-dione.

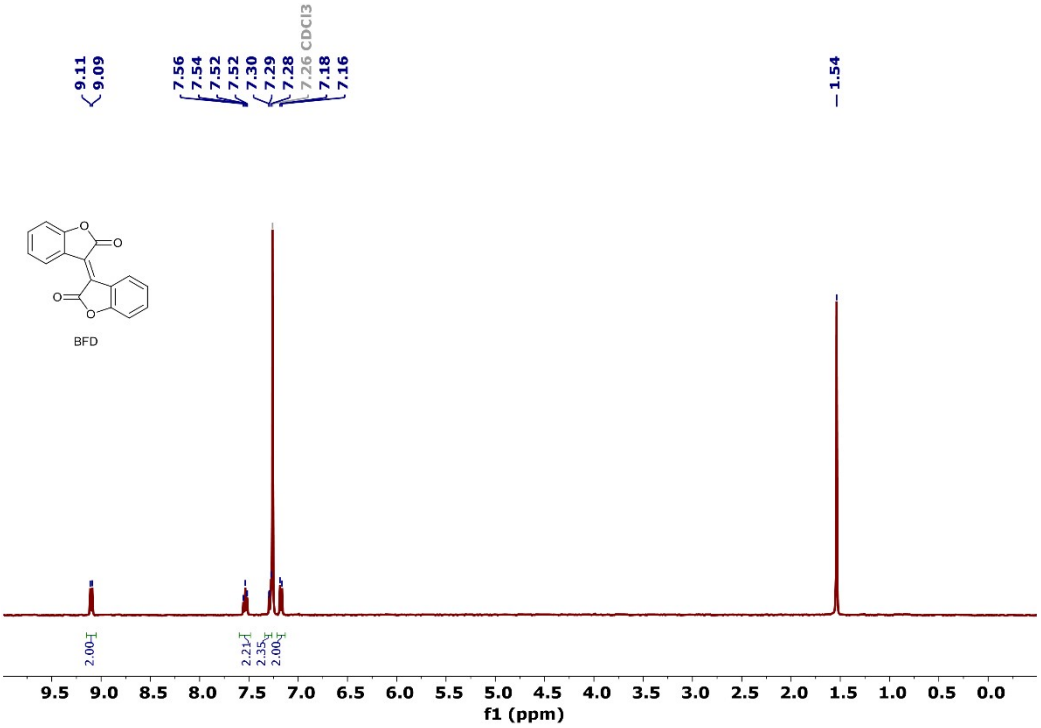

Fig. S25 ^{1}H NMR of (*E*)-2H,2′H-[3,3′-bibenzofuranylidene]-2,2′-dione (BFD).

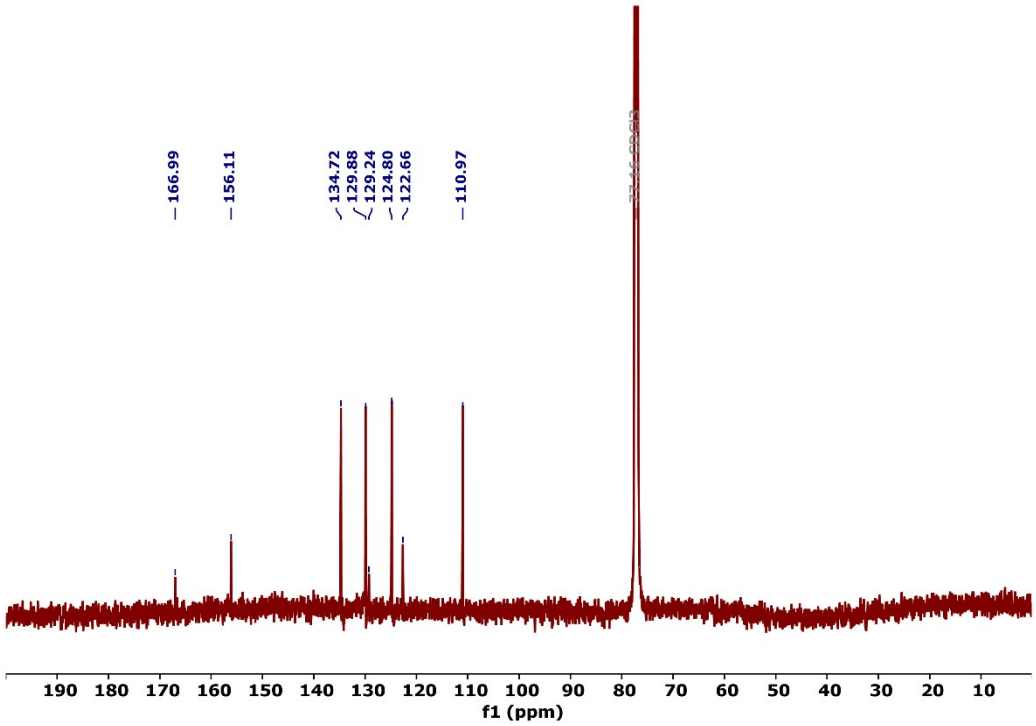

Fig. S26 ^{13}C NMR of (*E*)-2H,2′H-[3,3′-bibenzofuranylidene]-2,2′-dione (BFD).

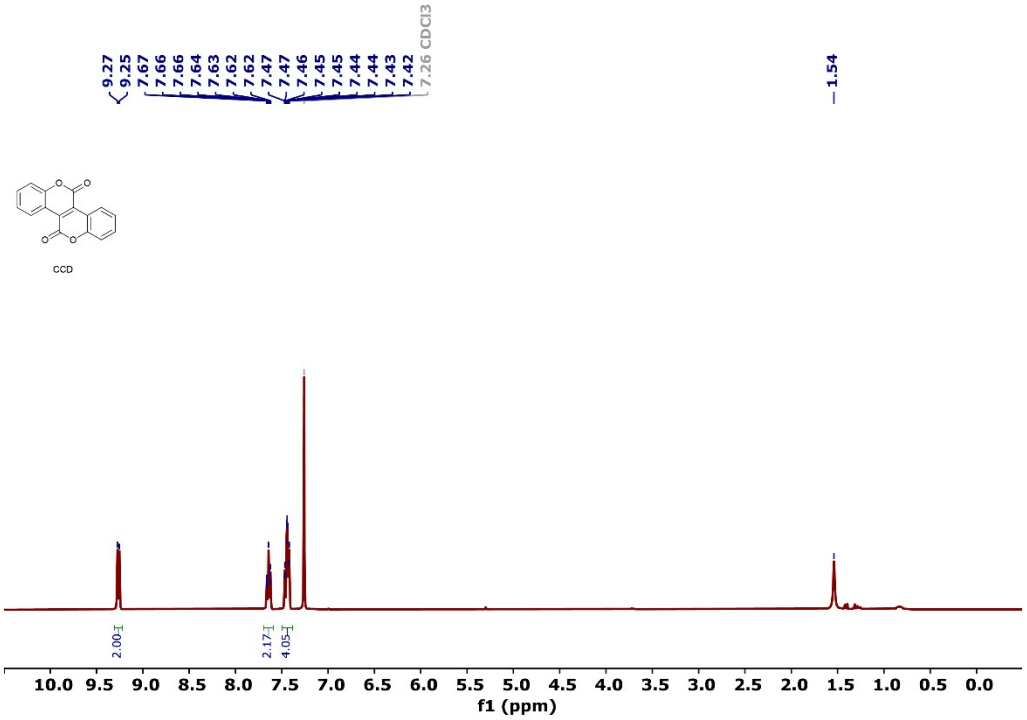

Fig. S27 ^{1}H NMR of CCD.

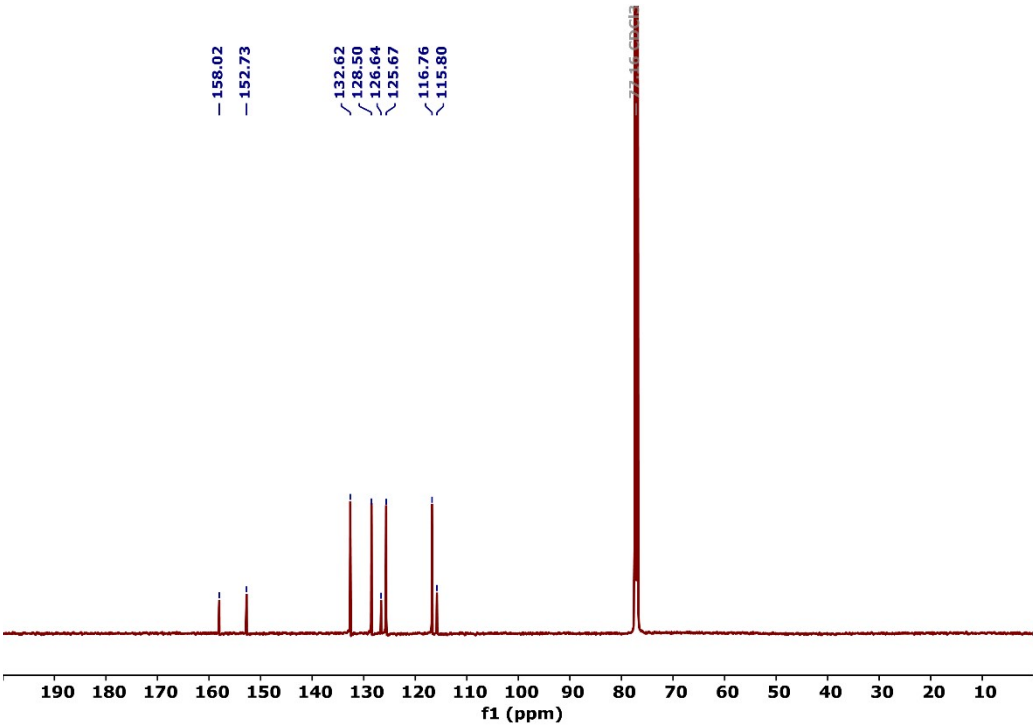

Fig. S28 ^{13}C NMR of CCD.

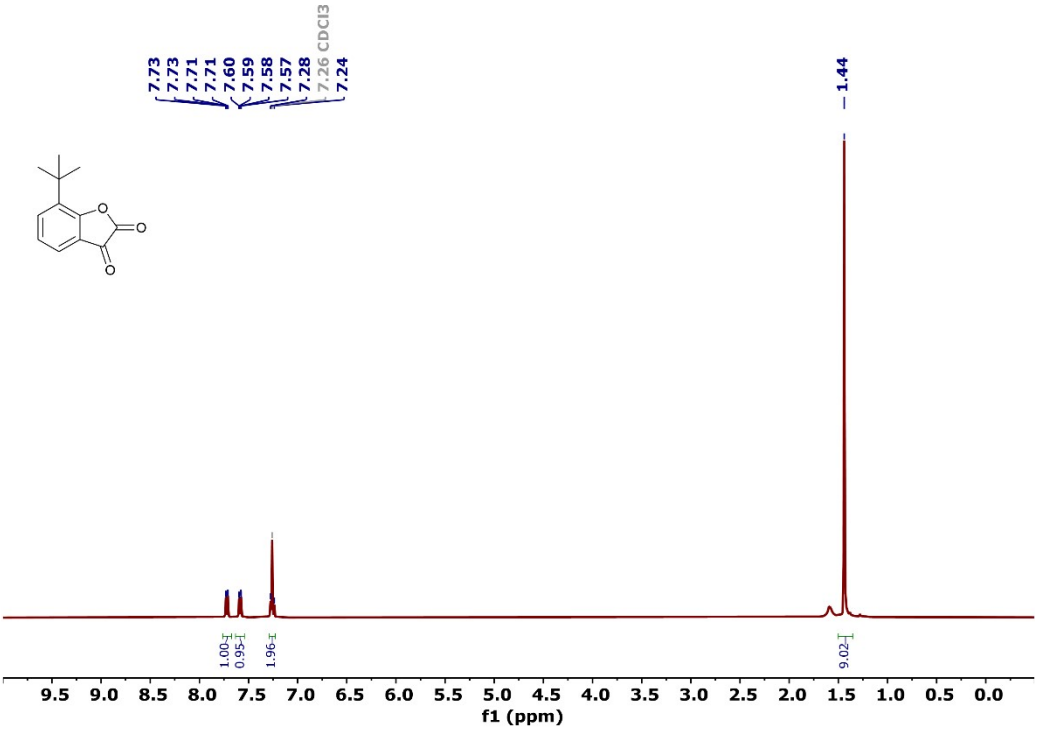

Fig. S29 ^{1}H NMR of 7-(*tert*-Butyl)benzofuran-2,3-dione.

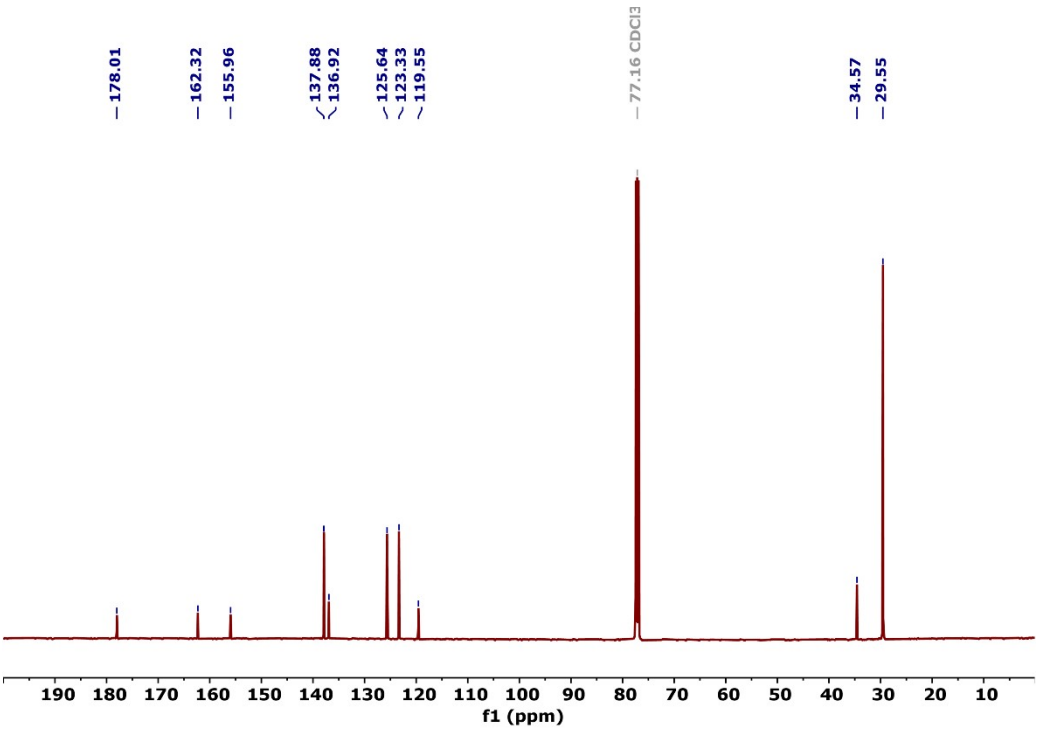

Fig. S30 ^{13}C NMR of 7-(*tert*-Butyl)benzofuran-2,3-dione.

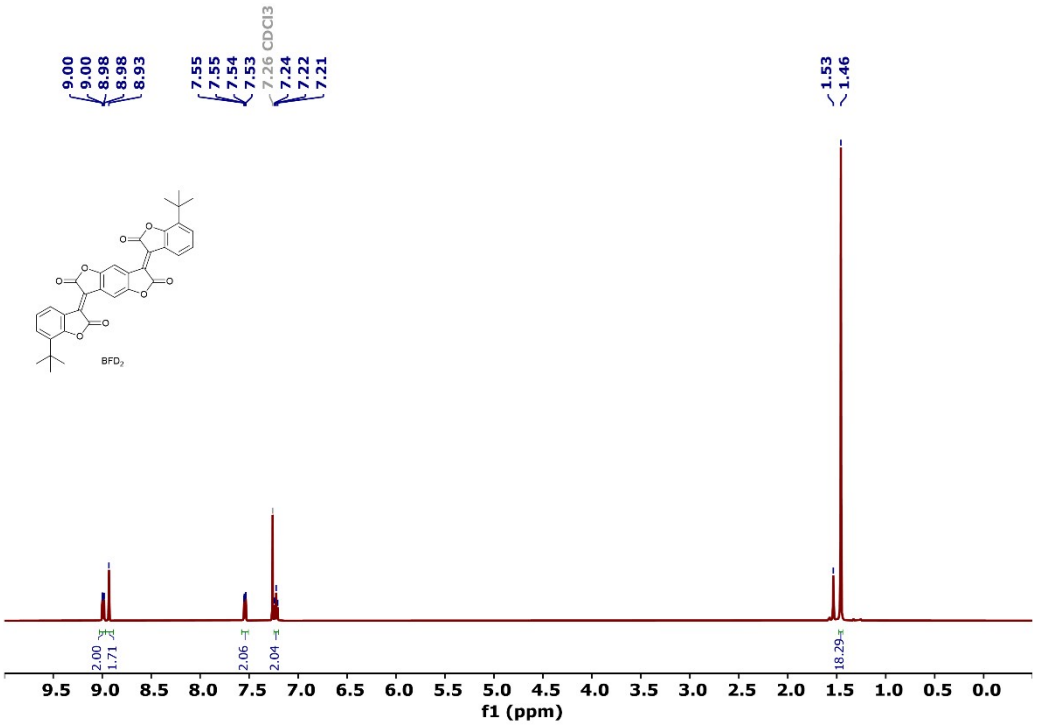

Fig. S31 ^{1}H NMR of BFD_2.

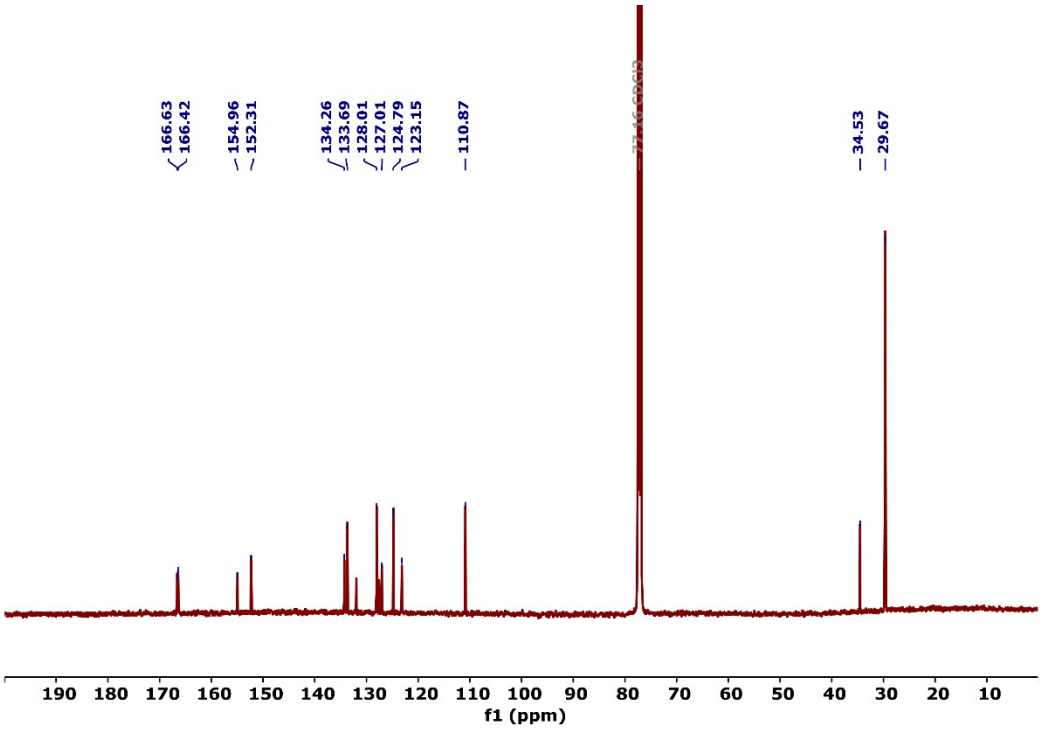

Fig. S32 ^{13}C NMR of BFD_2.

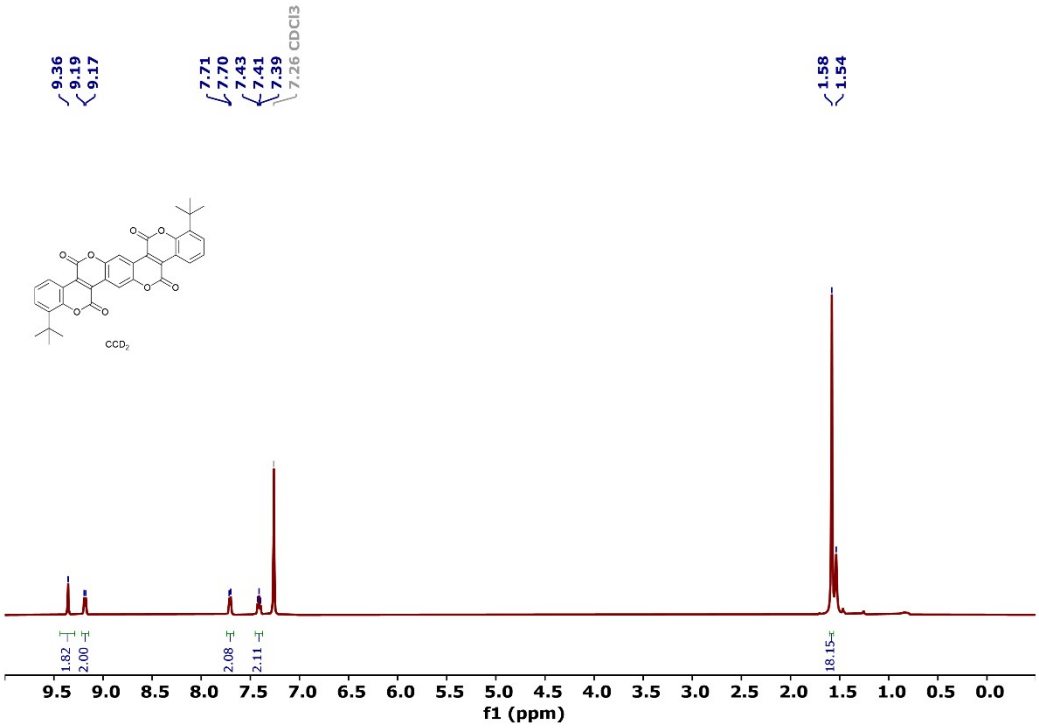

Fig. S33 ^{1}H NMR of CCD_2.

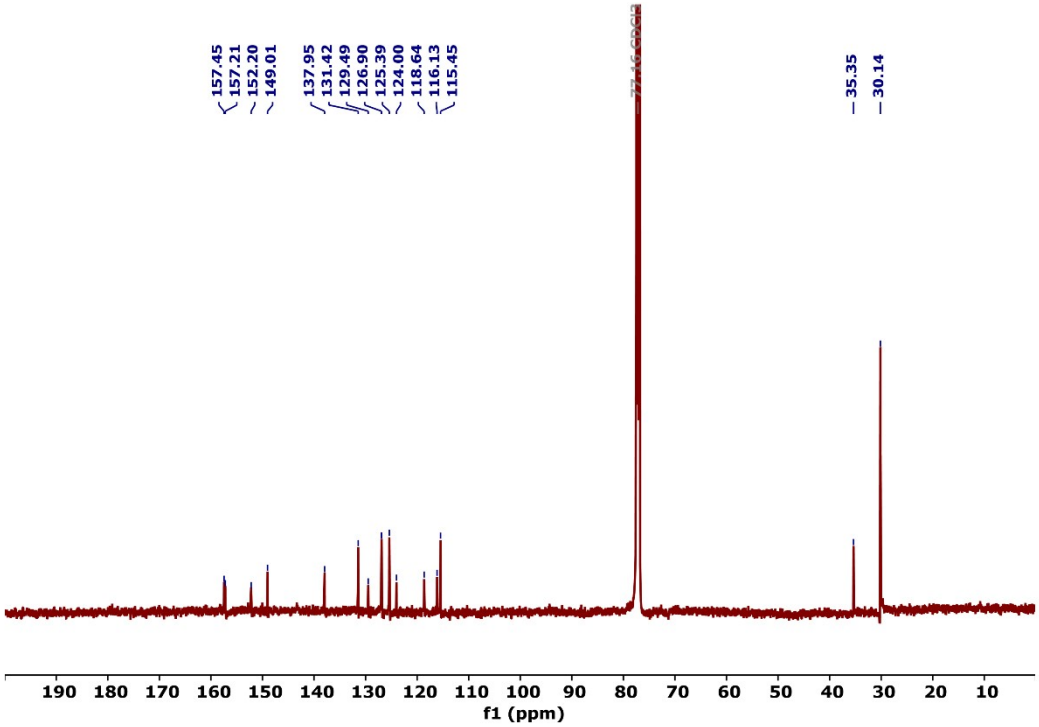

Fig. S34 ^{13}C NMR of CCD_2.

References

1 G. Liu, U. Pal, S. Samal, M. F. Espenship, Y. Li, W. Lee, L. A. Ogunfowora, L. You, J. Laskin and J. Mei, *Angew. Chem. Int. Ed.*, 2025, **64**, e202510411.

2 Z. Ke, A. Abtahi, J. Hwang, K. Chen, J. Chaudhary, I. Song, K. Perera, L. You, K. N. Baustert, K. R. Graham and J. Mei, *J. Am. Chem. Soc.*, 2023, **145**, 3706–3715.

3 M. H. Ahmed, J. Hwang, B. Xiao, M. R. Schiavone, J. Chaudhary, M. Chen and J. Mei, *Macromolecules*, 2024, **57**, 10717–10724.

4 H. Tang, Y. Liang, C. Liu, Z. Hu, Y. Deng, H. Guo, Z. Yu, A. Song, H. Zhao, D. Zhao, Y. Zhang, X. Guo, J. Pei, Y. Ma, Y. Cao and F. Huang, *Nature*, 2022, **611**, 271–277.

5 H. Un, S. A. Gregory, S. K. Mohapatra, M. Xiong, E. Longhi, Y. Lu, S. Rigin, S. Jhulki, C. Yang, T. V. Timofeeva, J. Wang, S. K. Yee, S. Barlow, S. R. Marder and J. Pei, *Adv. Energy Mater.*, 2019, **9**, 1900817.

6 Z. Ke, J. Chaudhary, L. Q. Flagg, K. N. Baustert, A. O. Yusuf, G. Liu, L. You, K. R. Graham, D. M. DeLongchamp and J. Mei, *Adv. Funct. Mater.*, 2024, **34**, 2400255.

7 S. Y. Son, G. Lee, H. Wang, S. Samson, Q. Wei, Y. Zhu and W. You, *Nat. Commun.*, 2022, **13**, 2739.